UNIVERSITY OF KWAZULU-NATAL ™

INYUVESI YAKWAZULU-NATALI

HMG-CoA Reductase Inhibitor, Atorvastatin, Induces Apoptosis in Human Lung Adenocarcinoma Cells (A549)

By

Pritika Ramharack

B.Sc. B. Med. Sc. (Hons) (UKZN)

Submitted in fulfilment of the requirements for the degree of M. Med. Sci

in the Discipline of

Medical Biochemistry and Chemical Pathology

School of Laboratory Medicine and Medical Sciences

College of Health Sciences

University of KwaZulu-Natal

Durban

2015

DECLARATION

This dissertation contains the original work by the author and has not been submitted in any form to another university. The use of work by others has been duly acknowledged in the text. The research described in this study was carried out in the Division of Medical Biochemistry and Chemical Pathology, School of Laboratory Medicine and Medical Science, Faculty of Health Sciences, University of KwaZulu-Natal, Durban, under the supervision of Prof. A.A. Chuturgoon and Miss S. Nagiah.

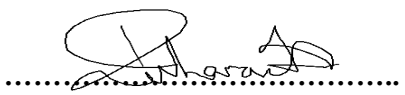

Miss P. Ramharack

AKNOWLEDGEMENTS

My family:

To my parents, my love and respect for you both are as great as the universe. Your trust and prayers have seen me through sleepless nights and painful days away from you. You provided for me even if it meant you having nothing for yourself. Your sacrifices will never be forgotten. To my Late Grandfather, no words can describe how much you are dearly missed. You have been my pillar of strength through all my endeavours, a role model that I looked up to and I am sure your guidance will be eternal.

Professor A.A Chuturgoon

I would like to thank you for accepting me into your prestigious department and for your guidance and support throughout my studies.

Miss S. Nagiah

I am grateful for all your assistance, supervision and guidance. Your dedication to fellow students and your work ethic is encouraging and I wish you all the best for the future.

The Masters students of 2015 in the discipline*:*

Thank you for all for the laughs, debates and for assistance throughout the year. The memories shall be forever a reminder of the friendships made.

The PhD students and staff in the discipline of Medical Biochemistry

Miss D.B. Naidoo, Mrs R. M. Myburg and Miss C.Tiloke, your unwavering support and friendship has carried me through this year and will always be cherished.

My Loved ones and Friends:

My friends who have become my family through the years. Every laugh, cry and smile we have shared is treasured. I could not have asked for better group of people to share these years with.

Nishall, your daily support and well wishes are what kept me motivated through even the rainiest days, thank you.

University of KwaZulu-Natal College of Health Sciences and National Research Foundation

Financial support as postgraduate student

PRESENTATIONS

Atorvastatin triggers ROS-induced Apoptosis in Human Lung Adenocarcinoma Cells (A549).

P. Ramharack, S. Nagiah and A.A. Chuturgoon.

UKZN College of Health Science research symposium (September 2015), Durban, South Africa.

LIST OF ABBREVIATIONS

Apaf-1	Apoptotic protease activating factor-1
ARE	Antioxidant response elements
ATM	Ataxia telangiectasia mutated
ATO	Atorvastatin
ATP	Adenosine triphosphate
BCA	Bicinchononic acid
BER	Base excision repair
BIR	Baculoviral IAP repeat
BSA	Bovine serum albumin
cDNA	Complimentary DNA
CCM	Complete culture medium
CHK2	Checkpoint kinase 2
Cu+	Cuprous ion
Cu2+	Cupric ion
DISC	Death inducing signalling complex
DMSO	Dimethyl sulphoxide
dNTP	Deoxynucleotide triphosphate
EDTA	Ethylenediaminetetraacetic acid
ELISA	Enzyme-linked immunosorbent assay
ER	Endoplasmic reticulum
ETC	Electron transport chain
FADD	Fas associated protein with death domain
$FADH_2$	Flavin adenine dinucleotide
FFP	Farnesylphosphate
GPP	Geranylphosphate
GPx	Glutathione peroxidase
GSSG	Glutathione disulphide
GST	Glutathione-S-transferase

h	Hours
H	Hydrogen
H_2O_2	Hydrogen peroxide
HMGCR	3-hydroxymethyl-3-glutaryl Coenzyme A reductase
HRP	Horseradish peroxidase
IAP	Inhibitor of apoptosis protein
IC_{50}	Half maximal inhibitory concentration
KEAP1	Kelch-like-ECH-Associated protein 1
LMPA	Low melting point agarose
MDA	Malondialdehyde
Mdm2	Mouse double minute 2 homolog
MMP	Matrix Metalloproteinase
mRNA	Messenger ribonucleic acid
mt	Mitochondria/mitochondrial
MPTP	Mitochondrial Permeability Transition Pore
MTT	3-(4, 5-Dimethyl-2-thiazolyl)-2, 5-diphenyl-2H-tetrazolium bromide
NADH	Nicotinamide adenine dinucleotide
NSCLC	Non-Small cell lung cancer
Nrf2	nuclear erythroid factor 2
OGG1	8-oxoguanine glycosylase
PARP-1	Poly (ADP-ribose) polymerase-1
PBS	Phosphate buffer saline
PERP	P53 apoptosis effector related to PMP-22
PI3K	Phosphoinositide 3-kinase
PTEN	Phosphate and tensin homology
Q-PCR	Quantitative polymerase chain reaction
RBD	Relative band density
RLU	Relative light unit
RNA	Ribose nucleic acid
ROS	Reactive oxygen species

RT	Room temperature
RTK	Receptor tyrosine kinase
SCGE	Single cell gel electrophoresis
SCLC	Small cell lung cancer
SDS-PAGE	Sodium dodecyl sulphate - polyacrylamide gel electrophoresis
SEM	Standard error of the mean
SH	Thiol
Smac/DIABLO	Second mitochondria-derived activator of caspases/DIABLO
SREBPs	Sterol regulatory element binding proteins
TBA/BHT	Thiobarbituric acid/ butylated hydroxytoluene
TBARS	Thiobarbituric acid reactive substances
TBST	Tris buffer saline tween 20
TCA cycle	Tricarboxylic acid cycle
TNF-α	Tumour necrosis factor-α
TRADD	Tumour necrosis factor –receptor 1 associated protein with death domain
USA	United States of America
XIAP	X-linked mammalian inhibitor of apoptosis protein

LIST OF FIGURES

LIST OF TABLES

TABLE OF CONTENTS

ABSTRACT

Atorvastatin (ATO) belongs to the statin family of drugs and is widely used for reducing cholesterol levels in cardiovascular disease patients. The target of statin drug therapy is the 3-hydroxymethyl-3-glutaryl Coenzyme A reductase (HMGCR) - a key rate-limiting regulatory enzyme in the mevalonate pathway for cholesterol synthesis. The end products of the mevalonate pathway are required for essential cellular functions, including membrane integrity, protein synthesis as well as cell proliferation and transformation. Recent evidence shows ATO to have a range of pleiotropic effects that includes anti-cancer properties. The antiproliferative effects of ATO was investigated on A549 lung carcinoma cells. Cell viability and ATP levels were measured by the 3-(4, 5-Dimethyl-2-thiazolyl)-2, 5 diphenyl-2H-tetrazolium bromide (MTT), LDH and ATP CellTitre-Glo™ assays, respectively. Cellular oxidative status was evaluated using the Thiobarbituric acid reactive substance (TBARS) and Glutathione (GSH) assays. Caspases-3/-7, -8 and −9 activities (luminometry) were determined and DNA integrity was assessed via comet and Hoechst 33342 staining assays. Quantitative polymerase chain reaction (qPCR) measured cellular mRNA levels of DNA repair enzyme, *OGG1*. The expression of proteins, namely, p53, bax, Bcl-2, Smac/DIABLO, cleaved-PARP and Nrf2 were evaluated by western blotting. ATO caused a dose-dependent decrease in cell viability (IC_{50} of 39.25µg/ml), a significant increase in extracellular LDH levels (p=0.0051) and significantly decreased cellular ATP levels (p=0.0003) whilst significantly increasing lipid peroxidation (p=0.0051) and decreasing GSH levels (p=0.0010). DNA integrity was compromised as measured by increased DNA fragmentation (p<0.0001) and significantly reduced *OGG1* mRNA expression (p=0.0363). Also PARP-1 cleavage was increased (24kDA fragment; p=0.0399). ATO induced apoptosis by significantly increasing caspase -8 (p=0.001), −9 (p=0.0143), and -3/-7 (p=0.0187) activities. Further, ATO increased expression of pro-apoptotic proteins Bax, p53 and Smac/DIABLO (p=0.0333; 0.0070; 0.0095) with a concomitant decrease in Bcl-2 and Nrf2 expression (p=0.03039; 0.0102). In conclusion, the data shows that ATO is a potent inducer of apoptosis (via both the intrinsic and extrinsic apoptotic pathways) in the A549 lung cells. Finally, ATO may hold promise as a chemotherapeutic drug for lung cancer.

CHAPTER 1:
1.1 INTRODUCTION

Lung cancer is the most common malignancy worldwide, with a high mortality rate, with approximately 1.61 million new cases diagnosed each year (Molina, 2008, Mukansi, 2014). The incidence of mortality in South Africa (SA) is estimated at 17% of all cancer-related deaths (Pacella-Norman, 2002).

Urbanization and lifestyle changes have seen an increase in the incidence of diseases such as lung cancer and cardiovascular disease. Tobacco smoking has been shown to increase both lung cancer and cardiovascular disease two-fold compared to non-smokers. The effect of the smoke directly inhaled predispose smokers to lung cancer, while absorption of toxic constituents or metabolites of smoke contribute to cardiovascular disease (Stein, 2008, Higgenbottam, 1982).

Conventional cancer treatment regimens such as chemotherapy are expensive and can produce acute and chronic organ damage. Thus, it has become necessary to identify improved strategies for cancer treatment and prevention (Siegel, 2012). In recent years, the development of molecular targeted therapeutics have evolved over common cytotoxic drugs. Many targeted agents that modulate specific oncogenic proteins have been approved or that are still under development with the hope to achieve better anticancer activity with fewer side effects. However, the ability of the tumour to counterattack these agents is still common, thus, combination regimens have become well-established to circumvent cancer resistance (Yu, 2006, Cassileth, 1996).

Statins are low molecular weight drugs derived from fungal fermentation and primarily used in the treatment of hypercholesterolaemia and cardiovascular disease. Statins reduce intracellular synthesis of cholesterol and in turn, decrease atherosclerotic plaque formation (Hindler, 2006, Rignanti, 2011). The mechanism of action of statins are to competitively inhibit the enzyme 3-hydroxymethyl-3-glutaryl Coenzyme A reductase (HMGCR), which converts HMG-CoA into mevalonic acid, a cholesterol precursor in the mevalonate pathway (Stancu, 2001). Statins act in a dose dependent manner to compete and alter the conformation of HMGCR, and prevent it from attaining a functional structure.

Atorvastatin (ATO) belongs to the statin drug family and is one of the most prescribed drugs to hypercholesteroleamic patients. Recent studies have shown that statins, including ATO, exert cholesterol-independent activity including anti-cancer properties. These effects can be explained by the drugs' main function in which they target and inhibit 3-hydroxy-methylgluraryl CoA reductase. This inhibition eventually leads to the reduced levels of many downstream products

of the mevalonate pathway which play pivotal roles in various cellular signalling pathways (Wong, 2002). Statins have proven to trigger cancer cell death in various tumour cells both *in vitro* and *in vivo* (Hoque, 2008, Hindler, 2006, Wong, 2002), thus creating new avenues in cancer therapeutics.

A hallmark of cancer is the evasion of apoptosis, cell survival and proliferation. These are seen by alterations and mutations in key regulators of apoptosis (Cairns, 2011, Wong, 2011). ATO has been shown to have synergistic interactions with drugs such as valproic acid (Barros, 2013) and gefitnib (Chen, 2013) which induce cell death in malignant cells, however, a clear mechanism of cell death in lung carcinoma has not been elucidated.

This study was designed to explore the cytotoxic effects of ATO on human lung adenocarcinoma cells (A549) by investigating molecular events contributing to cell death following acute exposure (48 hours) to the commercially used statin, ATO. It was hypothesised that ATO induces apoptotic death in cancerous lung cells, thus having dual therapeutic potential in hypercholesterolaemia and cancer.

1.2 LITERATURE REVIEW

1.2.1 Lung Cancer

1.2.1.1 Epidemiology

Lung cancer is the most common malignancy worldwide and has the highest mortality rate among cancers worldwide with approximately 1.61 million new cases each year (Molina, 2008, Mukansi, 2014). The mortality rate in South Africa is estimated at 17% of all cancer-related deaths and the risk of developing lung cancer is 1 in 20 for black South African males and 1 in 76 for black South African females (Pacella-Norman, 2002). A study on lung cancer completed in Johannesburg, South Africa, showed that adenocarcinoma was the second most common malignancy found in black males and white females. Studies also show that the disease is more common in men than in women with an estimated ratio of 2:1 (Mukansi, 2014).

The two most common types of lung cancer includes small cell lung cancer (SCLC) and non-small cell lung cancer (NSCLC). NSCLC has the highest incidence accounting for approximately 85% of diagnosed lung cancers (Molina, 2008). NSLC is made up of different cancer cells including squamous cell carcinoma, large cell carcinoma and adenocarcinoma.

In the search for cancer prevention and treatment, biomedical research requires the use of cancerous cells or tumours in order to identify accurate results. However, the use of patient tissue samples have increasingly stringent ethical and medical requirements. Thus *in vitro* models have been developed for the experimental studies worldwide. Human derived cell lines have been established to minimize the use of patient tissue samples in the developmental stages of testing compound (Gazdar, 2010).

The A549 cell line was established in 1972 and is derived from human lung adenocarcinoma cells. The cells may be characterised by type II pulmonary epithelium containing lamellar bodies which has allowed the cell line to be frequently used in toxicology and cancer therapeutic studies (Foster, 1998).

1.2.1.2 Risk factors

Urbanization as well as lifestyle changes have be associated with the increased incidence of lung cancer. Pollution, lack of physical activity and dietary changes have been the catalyst to cancer cell metabolism and proliferation (Molina, 2008). The 20th century has seen the emergence of a lung cancer epidemic in which cigarette smoking has played a central role. Studies have shown that tabacco smoking caused approximately 1.6 % of lung cancers and

passive smoking more than doubles the risk of lung cancer in adulthood. Cigarette smoke contains a complex mixture of carcinogens such as 4-(methylnitrosamino)-1-(3-pyridyl)-1-butanone (NNK) nicotine, benzo(a)pyrene, cadmium, and vapours such as formaldehyde and ethylcarbamate which can negatively affect cells of the respiratory system (Sexton, 2008).

Air pollution as well as occupational exposure to hazardous chemicals and carcinogens including polycyclic aromatic carbons and crysotile asbestos increase the risk of developing lung cancer through oxidative stress, inflammation and the deregulation of the nervous system (Pacella-Norman, 2002). Some incidences of lung cancer have been reported repeatedly within a family for over 60 years indicating a hereditary basis for the development of the disease. An increased risk of lung cancer was seen in TP53 germline sequence carriers and epidermal growth factor receptor T790M sequence variations (Molina, 2008).

1.2.1.3 Treatment

The treatment methods for lung cancer depends on the stage of development of the tumour and the availability of treatment methods. The most common conventional treatments include surgery and radiation for early stage cancer before metastasis occurs. The tumour cells may also develop resistance to treatment over a prolonged use. Anti-angiogenesis agents and receptor tyrosine kinase (RTK) inhibitors are a new targeted therapy which has shown improved response rates to different groups of patients with NSCLC (Molina, 2008, Cetintas, 2012).

Advanced stage cancer patients may undergo palliative chemotherapy (Molina, 2008). Systemic anti-cancer therapies, such as chemotherapy, can produce acute and chronic organ damage. Chemotherapy targets active cancerous cells, but are also lethal to healthy cells including bone marrow suppression as well as ocular, hepatic, cardiac and renal toxicity (Verhoef, 2008). New treatment regimens attempt to combat these harmful effects by providing therapy that involves aggressive, specific cancer cell death with minimal side effects to the patient (Cassileth, 1996). Chemoprevention agents such as dietary supplementation and plant-derived drugs may be used in combination with advanced chemotherapeutic drugs to produce a synergistic effect, thus enhancing the anticancer activities. Since recurrence of cancer after chemotherapy often occurs, new therapies would have to prevent the relapses, delay metastasis, and inhibit any chance of tumour growth (Mehta, 2014).

1.2.2 Statins

Statins are a class of drugs with a low molecular weight. These drugs are primarily used to treat patients diagnosed with hypercholesterolemia and cardiovascular disease. Statins reduce the

intracellular synthesis of cholesterol and in turn, decrease atherosclerotic plaque formation and stabilize pre-existing atherosclerotic plaques (Hindler, 2006, Rignanti, 2011). Statins are able to inhibit the conversion of HMG-CoA to mevalonate due to their action as structural analogues of HMG-CoA reductase (Istvan, 2001)

1.2.2.1 Pharmacology

Statins derived from fungal fermentation include lovastatin, simvastatin and pravastatin whereas the synthetic statin products include fluvastatin and atorvastatin (Figure 1.1) (Chan, 2003). The liver is the target organ for these drugs and the bioavailability is limited by extensive first pass metabolism. The Cytochrome P_{450} (CYP_{450}) monooxygenases are located in the endoplasmic reticulum (ER), with the liver and small intestine having the highest concentration of CYP_{450} enzymes. The enzymes allow for the oxidative metabolism of a wide range of compounds including medications. The CYP_{450} enzymes allow for the biotransformation of statins to polar compounds, making excretion possible via the kidney (Guengerich, 1993). The CYP_{450} pathways lead to the majority of statins having elevated serum levels, with lovastatin, simvastatin and atorvastatin primarily being oxidized by CYP_{450} 3A4 (Stancu, 2001, Chan, 2003).

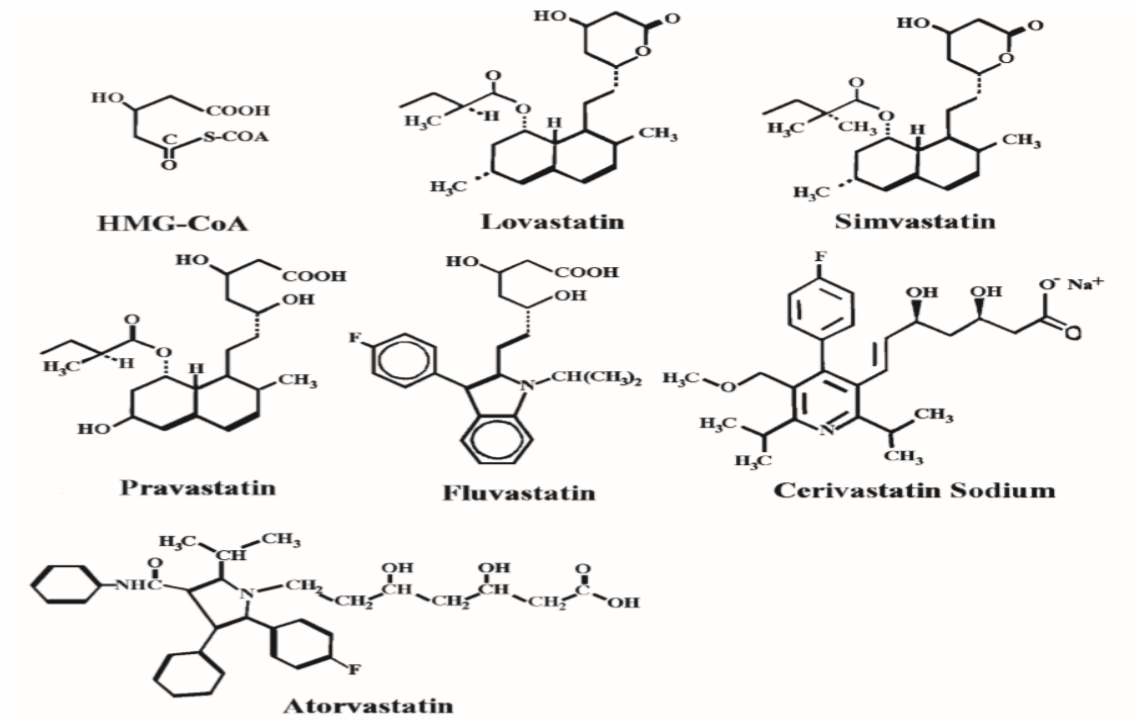

Figure 1.1: Chemical structures of HMG-CoA reductase inhibitors (statins). Simvastatin, lovastatin, and pravastatin are derivatives of fungal products as they have a hydronaphthalene ring in common, whereas fluvastatin, cervastatin and atorvastatin are chemically synthesized (Stancu, 2001).

1.2.2.2 Mechanism of Action

Statins target hepatocytes and inhibit the enzyme HMGCR, which converts HMG- CoA into mevalonic acid, a cholesterol precursor in the mevalonate pathway (Stancu, 2001). Statins act in a dose dependent manner to competitively inhibit and alter the conformation of the HMGCR enzyme. This prevents the enzyme from attaining a functional structure, hence these drugs are very specific and effective. The inhibition of HMGCR eventually leads to the increase in hepatic low –density lipoprotein (*LDL*) and hence low circulating *LDL* (Figure 1.2). This occurs by inducing the splicing of sterol regulatory element binding proteins (SREBPs) by a protease from the ER. The SREBPs translocate to the nucleus where they induce gene expression for the *LDL* receptor. The decrease in cholesterol synthesis in hepatocytes leads to a negative feedback which increases hepatic *LDL* receptors which allows for the binding of *LDL* to these receptors, thus decreasing circulating *LDL* and its precursors (Stancu, 2001, Tandon, 2004).

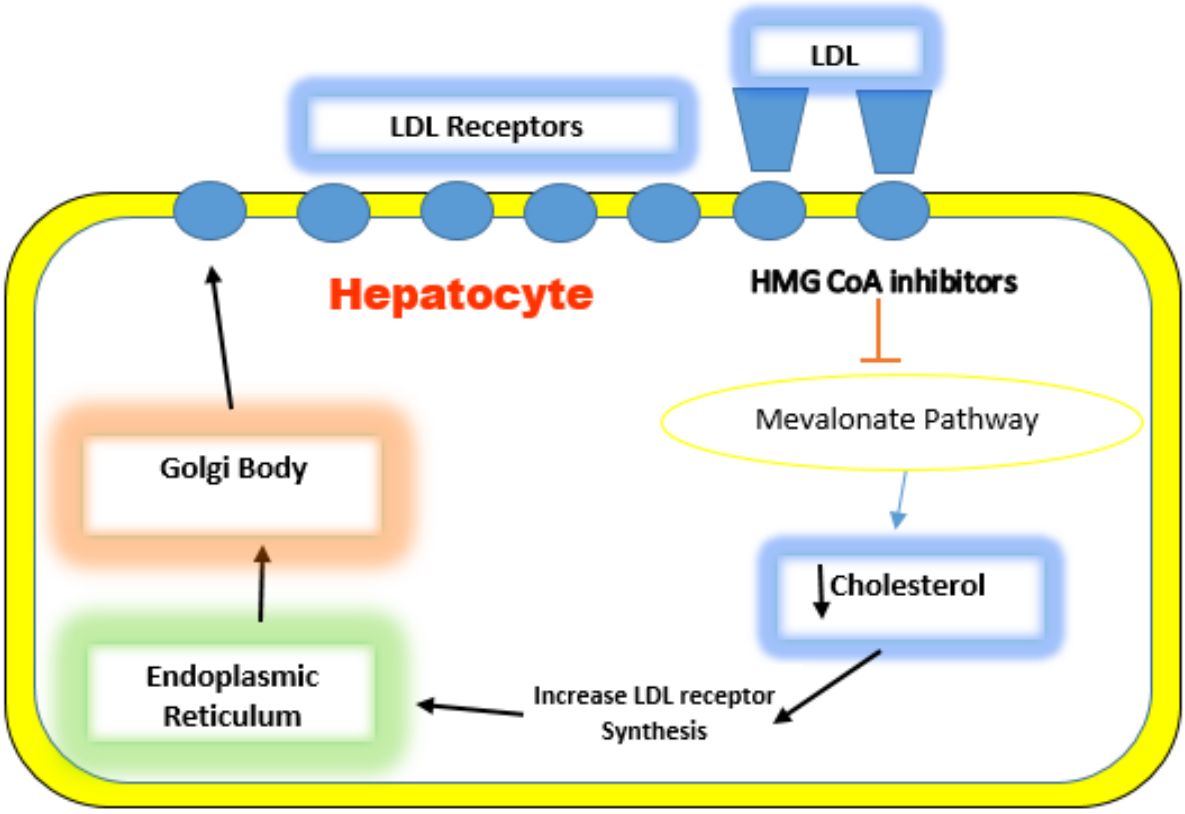

Figure 1. 2: Fate of LDL in hepatocytes after treatment with statins (Prepared by Author).

Statins not only reduce serum cholesterol levels but also mevalonate synthesis and isoprenoid metabolites (Figure 1.3) (Pisanti, 2014). This leads to decreased downstream products of the mevalonate pathway including dolichol, geranylphosphate (GPP) and farnesylphosphate (FPP). Geranylphosphate and farnesylphosphate play a role in a number of cellular processes by acting as lipophilic anchors on the cell membrane and allow for the attachment and biological activity of proteins from the GTPase family (Cafforio, 2005). G-proteins Ras and Rho are isoprenylated by GPP and FPP. These G-proteins are key regulators of signal transduction of membrane receptors involved in cell proliferation, differentiation and apoptosis (Rignanti, 2011). Studies have shown that Lovastatin stabilizes cell cycle kinase inhibitors p21 and p27 and leads to cell cycle arrest in the G1 phase in breast cancer cell lines. Dolichol has stimulatory effects on DNA synthesis and may interact with several tumour cell proteins (Hindler, 2006). Ubiquinone is one of the end products of the mevalonate pathway and functions in the production of ATP from the mitochondria (Chan, 2003).

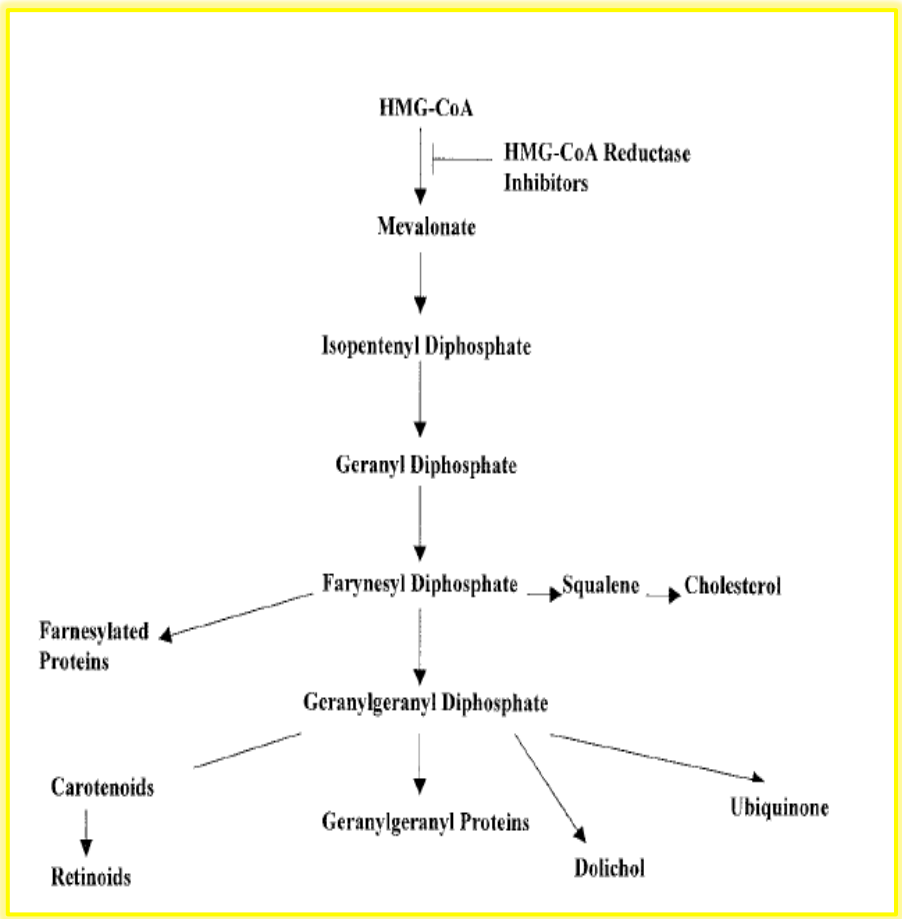

Figure 1.3: Mevalonate pathway products are reduced by the inhibition of HMG CoA reductase, leading to downstream metabolic effects of cells (Stancu, 2001).

1.2.2.3 Pleiotropic Effects of Statins

The lipid-lowering effects of statins are generally well known, however recent studies have shown that statin therapy may have other beneficial aspects independent of its cholesterol-lowering effects. Tandon *et al* (2001) expanded on the pleiotropic actions of HMG CoA inhibitors including its anti-inflammatory actions, its ability to reverse endothelial dysfunction by decreasing *LDL* oxidation and increasing nitric oxide (NO) availability. The drugs have also been shown to modulate vascular remodelling by the inhibition of transcription factors such as Nuclear Factor Kappa-B (NFkB) and cellular matrix metalloproteinases (MMP) (Hindler, 2006).

The mevalonate pathway for cholesterol synthesis has been implicated in tumorigenesis, with studies in the past decade looking at statins as therapeutic agents in cancer by researching the anti-proliferative effects of statins with regard to cell cycle arrest and apoptosis (Pisanti, 2014).

Stancu *et al* (2001) described the effect statins have on osteoclast formation and bone resorption, where recent experimentation showed that Lovastatin inhibited GTP- binding proteins which act to control cytoskeletal reorganisation, vesicle fusion and apoptosis, which are processes that are involved in osteoclast activation and survival (Stancu, 2001, Lee, 2006).

1.2.2.4 Adverse effects of Statins

Statins are generally well endured with the only toxicities observed being liver and muscle toxicity. Various hypotheses have been proposed to account for the muscle dysfunction related to statin use. Ubiquinone depletion leads to myalgia in patients on statin treatment (Chan, 2003). Myopathy can occur if there is co-administration of statins with inhibitors of CYP_{450} enzymes, other inhibitors of statins or inhibitors of statin metabolites. Fibrates and niacin also increase the risk of myopathy (Stancu, 2001). Statins have been reported to affect skeletal muscle membrane physiology by changing membrane fluidity, Na^+/K^+ pump density and change in cholesterol content. This may lead to changes in calcium concentration resulting in membraneolysis (Stancu, 2001, Chan, 2003).

Stroes *et al* (2015) elucidated on the deleterious effects of statin therapy on mitochondrial function. Biopsies of skeletal muscle from patients on statin therapy showed increased intramuscular lipid content, reduced mitochondrial DNA and lower mitochondrial oxidative phosphorylation during simvastatin use. Genetic susceptibility to statin-induced myopathy is a new research avenue that is being investigated (Stroes, 2015). A study on patients undergoing high-dose simvastatin showed that the protein encoded gene, SLCO1B1, which is associated with statin toxicity, detected a defective single nucleotide polymorphism (SNP), rs4149056, in disequilibrium with the c_521T_C SNP. It was seen that in homozygotes, the SNP was

associated with an 18% risk of muscle symptoms compared with heterozygotes, in those without risk alleles, the risk of muscle symptoms were 0.6% (Stroes, 2015).

1.2.3 Statins: Potential in Cancer Therapy

Statins have been well described to be anti-atherosclerotic, anti-thrombic and anti-inflammatory in both *in vitro* and *in vivo* models. Hindler *et al* (2006) suggested that statins may also have anti-proliferative, anti-angiogenic and anti-metastatic properties which would lead to a novel therapeutic approach to cancer treatment and even prevention (Hindler, 2006).

In recent years, increasing evidence from *in vitro* and *in vivo* studies have established the anti-tumour activity of statins, independent of cholesterol reduction. These anti-tumour properties have been seen in prostate (Lee, 2006), colon (Agarwal, 1999), leukaemic (Xia, 2001), pancreatic (Kusama, 2001) and breast cancer cells (Denoyelle, 2001). Studies have also been done on the effects of statins on normal cells. Gauthaman *et al* (2007) showed that cell proliferation of ovarian and colon cancer was inhibited by simvastatin, lovastatin, and mevastatin, whereas normal embryonic stem cell growth was not affected by all of these four statins (Gauthaman, 2007). Preclinical studies have demonstrated that lipophilic statins such as lovastatin and atorvastatin have better anti-tumour activity, relative to hydrophobic statins such as pravastatin. This is logical since lipophilic statins are more accessible to tumour cells (Cafforio, 2005).

Hoque *et al* (2008) showed that statins may trigger different tumour cells to undergo apoptosis *in vitro* and supress tumour growth *in vivo* (Hoque, 2008). This was also expressed by Hindler *et al* (2006) which described experiments where statins inhibited tumour growth and induced apoptosis in various malignancies including neuroblastoma, glioma and leukaemic cell lines (Hindler, 2006).

The reduction of sterol synthesis by statins suggest that inhibition of tumour growth may be related to the reduction of non-steroidal isoprenoid compounds. This inhibits Ras dependent tumour cell growth due to the decrease in farnesylphosphate production. Mevalonate also plays a key role in cell proliferation, and malignant cells have increased HMG CoA reductase activity (Stancu, 2001). This information suggests that statins can selectively inhibit tumour growth and could lead to a new chemotherapy agent.

1.2.3.1 The apoptotic effects of Statins:

Statins affect the lipid raft in the plasma membrane. These hydrophobic molecules are involved in signal transduction of processes such as migration, growth and survival. Hoque *et al* (2008) showed that statins were able to initiate apoptosis in different tumour cells *in vitro* and inhibited growth of tumours *in vivo*. Wong *et al* (2002) described tumour specific apoptosis due to statins after performing experiments on both primary and derived cell lines (acute myeloid leukemia (AML), myeloid progenitor cells from bone marrow and blood and non-transformed hematopoietic cells). Lovastatin induced apoptosis in the AML cells but the progenitor cells and non-transformed cells did not undergo apoptosis and retained their full proliferative potential (Wong, 2002).

Studies also show that statins mediate apoptosis by upregulating pro-apoptotic proteins such as Bax and Bim, and downregulate anti-apoptotic proteins Bcl-2 and Bcl-x. Lovastatin increased Bim protein expression and induced programmed cell death in glioblastoma cells, with similar effects on prostatic epithelium and leukaemic cells through the activation of caspases 3 and 7 (Hindler, 2006). Other studies showed apoptosis to be mediated through the depletion of GPP. Xia *et al* (2001) reported that mevalonate and GPP reversed the cellular apoptosis induction of lovastatin in acute myeloid leukaemia cells, indicating the inhibition of geranylgeranylation of target proteins is an important mechanism of lovastatin-induced apoptosis (Xia, 2001). Pisanti *et al* (2014) described the initiation of apoptosis via the inhibition of Ras-MAPK and PI3K/AKT pathways, thus regulating anti- and proapoptotic mRNA and protein levels (Pisanti, 2014).

1.2.3.2 The Anti-Proliferative effects of Statins

Chan *et al* (2003) elucidated that statins are able to synchronize tumour cells by blocking the transition in the cell cycle from the G1 to S phase. This was reversed by mevalonate. It was also found that the inhibition of cell growth by Lovastatin did not depend on Ras function (Chan, 2003). Recent studies have shown that cell cycle arrest is mediated by an increase in cyclin dependent kinase inhibitors, $p21^{waf1/AP1}$ and $p27^{KIP}$, in which degradation is reliant on Rho GTPases. Statins decrease the isoprenylation of Ras and Rho proteins due to the inhibition of GPP and FPP isoprenoids. Ras and Rho proteins are able to bind to and hydrolyse GTP and thus activate downstream effectors such as serine-theronine kinases, NFkB, Stress-activated protein kinases- jun amino-terminal kinases (SAPK-JNK), PI3K and Ras-MAPK pathways and eventually lead to cell proliferation. By the inhibition of Ras and Rho proteins, statins may thus be able to reduce tumour cell growth and inhibit cell proliferation (Rignanti, 2011, Cafforio, 2005).

The mevalonate pathway for cholesterol biosynthesis and protein prenylation has been found to initiate many aspects of tumour progression. Statins therefore play a beneficial role in cancer research. The optimal regimen for statin therapy however has not yet been defined. Statins, alone, are not effective anticancer agents, but in combination with other cytotoxic agents, preclinical as well as clinical data shows that statins may enhance the effect of chemotherapeutic agents (Hindler, 2006). In conclusion, it may be said that statins are the new stepping stone to cancer therapy.

1.2.4 Apoptosis: Programmed Cell Death

Daily billions of cells are subjected to programmed cell death in order to maintain optimal functioning of an organism. The regulation of the number of cells in these organisms are very important and follow a chain of events that finally lead to the process of apoptosis. Apoptosis was first described in 1972 (Kerr, 1972). Programmed cell death may be characterized by its distinct morphological characteristics as well as its energy-dependent nature. Apoptosis occurs through normal aging and development and can also occur as a defence mechanism in the immune system (Elmore, 2007).

A group of aspartate- specific cysteinyl proteases referred to as caspases execute apoptosis. These caspases are expressed as inactive zymogens that are proteolytically activated following a stimulus (Rastogi, 2009). There are two distinct groups, the initiator and activator caspases 2, 8, 9 or 10 which allow for the cleavage and activation of a second group of caspases being the effectors or executioner caspases 3 or 7 which allow for the initiation of apoptotic cascade (Johnstone, 2002, Fischer, 2006).

During the process of apoptosis, cell shrinkage is an early morphological feature. When the cell shrinks, it allows for the organelles to become tightly packed and the cytoplasm to become dense. Chromatin condensation is a common feature seen in apoptosis and is known as pyknosis. The plasma membrane then begins to form blebs and separate in apoptotic bodies. These bodies are then phagocytosed by macrophages and parenchymal cells and degraded within phagolysosomes (Elmore, 2007).

There are two major apoptotic pathways that exist in mammalian cells, the extrinsic death receptor-mediated pathway and the intrinsic mitochondrial/p53-mediated pathway (Figure 1.2). Both pathways require constant control and regulation and require a constant supply of energy for the cascade of molecular events (Elmore, 2007).

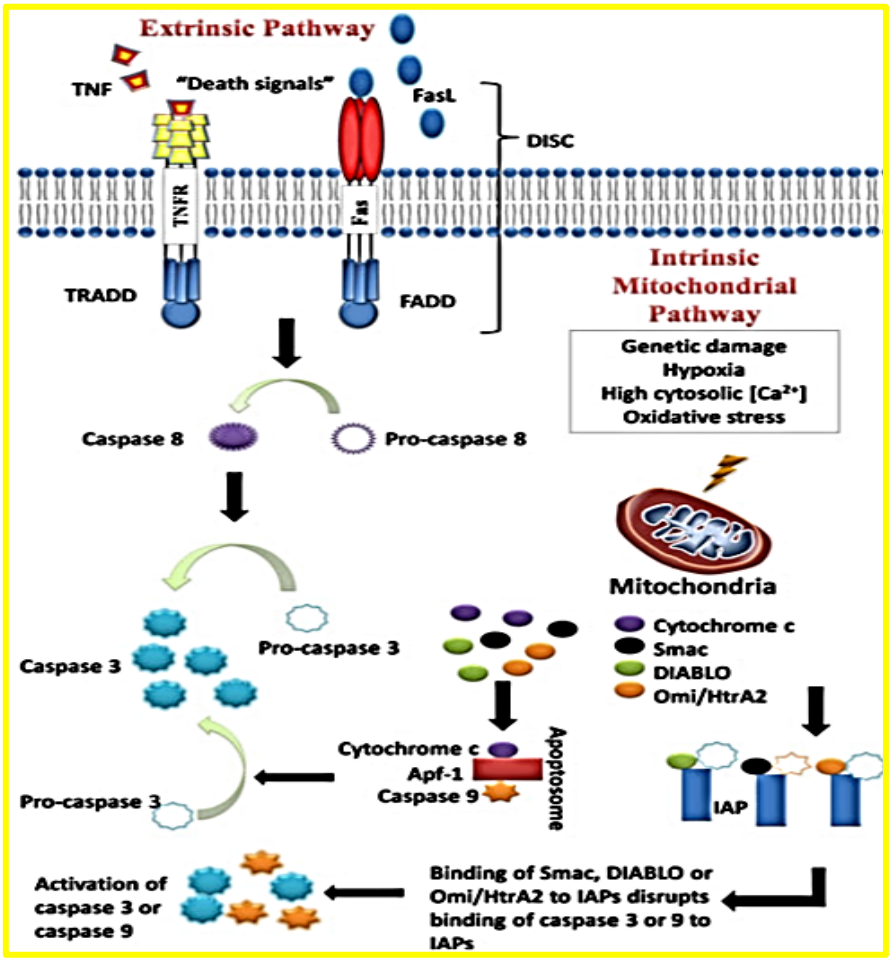

Figure 1.4: Overview of the extrinsic and intrinsic apoptotic pathways (Wong, 2011).

1.2.4.1 The Extrinsic Apoptotic Pathway

The extrinsic apoptotic pathway or death receptor pathway makes use of transmembrane death receptor-mediated reactions which involve the tumour necrosis factor (TNF) –α family of death receptors including CD95, TNF receptor and TRAIL receptor. Receptors of the family share a domain which is cysteine rich with a domain known as the death domain. The function of the death domain is to transfer death signals from the cell surface to the inside of the cell. Ligation of the transmembrane death receptors initiate this pathway. Fas-L/Fas R recruit Fas associated protein with the death domain FADD, TNF/TNF-R recruits TNF-R1 associated protein with the death domain TRADD with FADD. Dimerization of a death effector domain (DED) then occurs and FADD is able to communicate with procaspase 8 and form a death inducing signalling complex (DISC) which results in the cleavage and the activation of caspases 8. The executioner caspases are then activated and apoptosis is initiated (Fulda, 2006, Hsu, 1995, Johnstone, 2002).

Rastogi et al (2009) also mentioned FLIP as an inhibitory molecule in the activation of caspase 8. FLIP is a caspase 8 homolog that binds to FADD and caspase 8, rendering them inactive and inhibiting death receptor-mediated apoptosis (Rastogi, 2009).

1.2.4.2 The Intrinsic apoptotic Pathway

The intrinsic apoptotic pathway consists of a diverse series of intracellular mediators in which mitochondria play a significant role in, resulting in the activation of the caspase pathway and eventually leading to the execution phase of apoptosis and cell death (Fulda, 2006).

The permeabilisation of the inner mitochondrial membrane is a crucial step in the intrinsic pathway for the release of apoptotic proteins. The loss of mitochondrial transmembrane potential is due to the regulation of two Bcl-2 family members by transcription factor p53. P53 inhibits the anti-apoptotic protein Bcl-2 and activates cytosolic Bax, which becomes oligomerised and forms mitochondrial membrane permeability transition pores. The release of apoptogenic molecules, Cytochrome c and serine protease HtrA2/Omi then occur which brings about the formation of the apoptosome which is made up of Cytochrome c, apoptotic protease activating factor 1(Apaf1) and procaspase 9. Cytochrome c binds the closed inactive form of Apaf-1, forcing it into its open active conformation. This frees the N-terminus of Apaf-1, which is normally bound and inhibited by WD-40 repeat region, allowing Apaf-1 to bind and activate procaspase-9 (Fulda, 2009).The clustering of procaspase 9 leads to the activation of caspases 9 which in turn activate the executioner caspases (Elmore, 2007, Wang, 2001).

1.2.4.3 Caspase Independent Apoptosis:

Caspase independent apoptosis was first seen in the human Jurkat cell line, where the inhibition of caspases did not inhibit Bax-induced cell death but it did change the morphology of the dying cell (Broker, 2005). Evidence now shows that programmed cell death can occur in the absence of caspases and be induced by non-caspase proteases. Different cell organelles have been implicated in contributing to cell death in a caspase-independent manner with the mitochondria playing a central role by releasing death executors from the intermembrane space to the cytosol, triggering the death of the cell (Rieckher, 2010).

Other proteins involved in caspase-independent apoptosis include endonuclease G and Apoptosis inducing factor (AIF). Endonuclease G is a mitochondrial enzyme that is able to execute caspase-independent DNA fragmentation in nuclei. The enzyme is able to interact with DNase I to generate internucleosomal DNA fragments during oxidative stress conditions (Bajit, 2006). Another mitochondrial protein that plays an important role in apoptosis is AIF which is normally found in the intermembrane space of the mitochondria where it undergoes an oxidoreductase function. (Broker, 2005). Calpains are proteases that are normally found as

inactive zymogens in the cytosol but during ER stress, they are released and play a role in degradation of proteins (Figure 1.5).

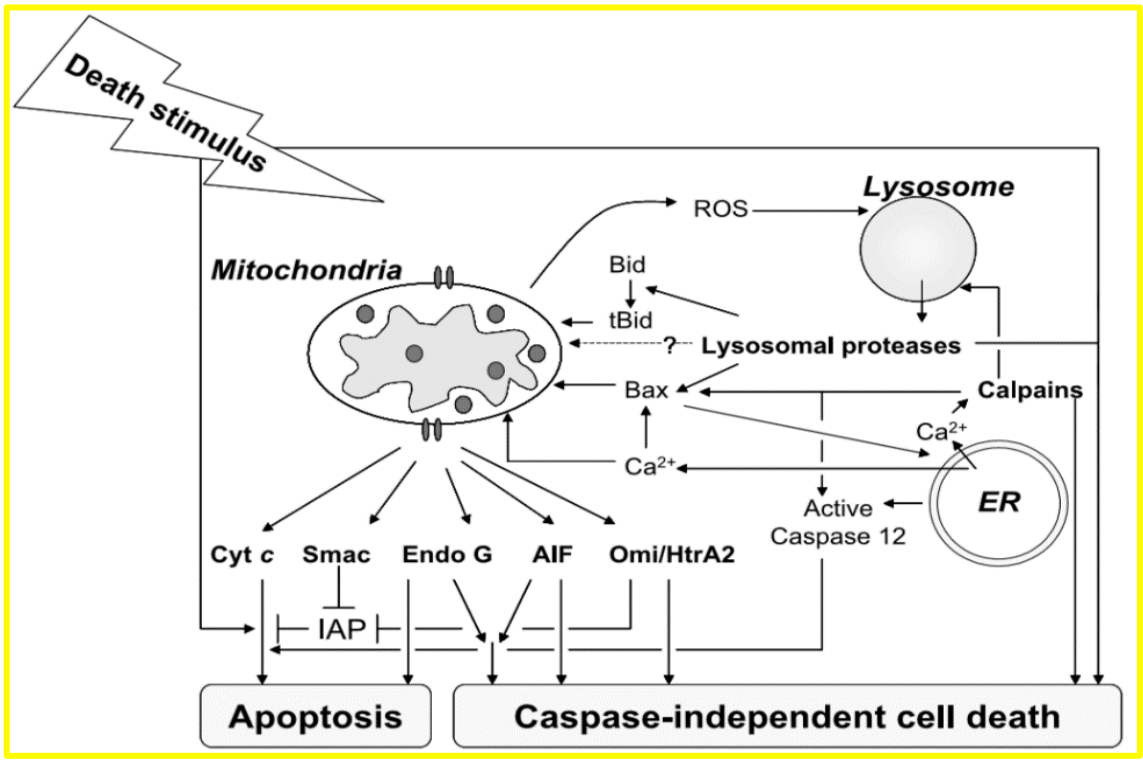

Figure 1.5: Crosstalk between organelles during cell death which may be triggered dependent (intrinsic apoptotic pathway) or independent of caspase (Broker, 2005).

1.2.4.4 P53 and Apoptosis

Transcription factors act to maintain tissue homeostasis and control the number of cells within an organism (Fridman, 2003). The p53 tumour suppressor protein has been extensively studied and found to be a regulator of many cellular processes including apoptosis. P53 halts the cell cycle to repair the damage to cell's DNA or allow for apoptosis during hypoxic conditions or mutagenic oncogene expression. Mutations in the TP53 gene lead to a mutant form of the gene that is unable to regulate cell growth and division effectively, thus resulting in the continued survival and proliferation of damaged cells. In cancer cells, this trait is well established as there is common dysregulation of the p53 transcription factor (Fridman, 2003).

Previous studies have described p53 as a mediator of cell fate depending on stress, cell type, tissue and other cofactors. The 'affinity model' was created to expand on the outcome of p53 activation and it proposed that low p53 levels bind to high affinity p53 response elements in

pro-arrest genes and vice versa where high levels of p53 is needed to bind to low affinity response elements in pro-apoptotic genes (Kracikova, 2013).

Approximately 50% of human cancers have p53 mutations but it is seen that the remaining 50% can elucidate p53 as a major target for anti-cancer drug development (Wang, 2012). Proteins that sense DNA damage such as Checkpoint Kinase 2(CHK2) and Ataxia telangiectasia mutated (ATM) phosphorylate and stabilize p53 and inhibit its mouse double minute 2 homolog (MDM2)-ubiquitination and degradation (Johnstone, 2002, Wang, 2012). P53 may be phosphorylated at different sites by multiple kinases. Phosphorylation of p53 at serine 46 regulates the ability of p53 to induce apoptosis, whereas phosphorylation at serine 392 regulates the cell cycle (Ashcroft, 1999).

P53 functions as a master regulator in the mitochondrial dependent apoptotic pathway by transcriptionally activating Bcl-2 proapoptotic proteins and inhibiting anti-apoptotic proteins such as Bcl-2 and IAPs (Figure 1.6). It can also transactivate other apoptotic proteins such as phosphatase and tensin homolog (PTEN), p53 apoptosis effector related to PMP-22 (PERP) and Apaf1 (Johnstone, 2002).

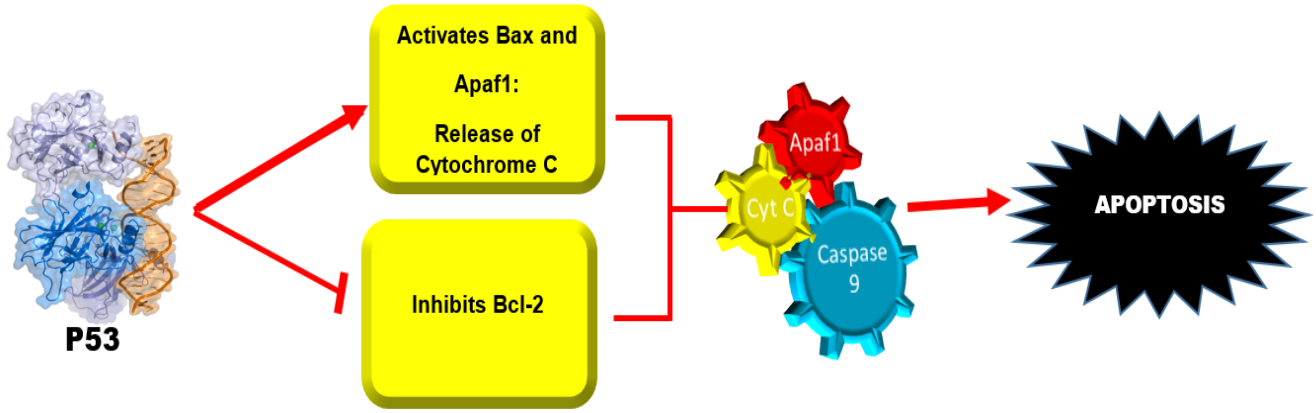

Figure 1.6: p53 regulation in the mitochondrial/ intrinsic apoptotic pathway (Prepared by Author).

1.2.4.5 Bcl-2 and Bax regulation of Apoptosis:

The Bcl-2 family of proteins act as key regulators of mitochondrial-dependent apoptosis and the mitochondrial outer membrane permeability pore. The Bcl-2 family are divided into three groups, the pro-apoptotic multidomain, anti-apoptotic/pro-survival proteins and the pro-apoptotic BH3 only proteins. All members of the family have one or more homology domains which are labelled as the Bcl-2 homology (BH 1, 2, 3 and 4). This homology allows for the interaction between the members of the family (Ola, 2011).

Bcl-2 is an anti-apoptotic or pro-survival protein that contains a carboxy-terminal hydrophobic transmembrane tail domain, this domain allows it to remain within the outer mitochondrial membrane. The protein acts to inhibit the characteristic features of apoptosis by inducing survival mechanisms by various stimuli which prevent mitochondrial outer membrane permeability. Bcl-2 also binds to and inactivates pro-apoptotic proteins to inhibit the downstream events of apoptosis. Bcl-2 associated X protein (Bax) is a proapoptotic protein that lies dormant in the cytosol by interactions with various proteins such as humanin peptides. The activation of Bax leads to the exposure of the N-terminus of the protein which cause a conformational change and the formation of homo-oligomers. These oligomers produce pores in the outer mitochondrial membrane and constitutes a change in mitochondrial membrane potential leading to the release of pro-apoptotic molecules from the formed pores (Ola, 2011, Elmore, 2007, Johnstone, 2002).

1.2.4.6 Smac/DIABLO regulation of Apoptosis:

Second mitochondria-derived activator of caspases/Direct inhibitor of Apoptosis-Binding Protein with Low pI (Smac/DIABLO) is a 25-kDa mitochondrial protein which is released from the mitochondria during apoptosis (Wang, 2001). This nuclear encoded protein is able to translocate into the mitochondria. During the transition, the N-terminus is removed by proteolysis, producing an activated form of the molecule. The activated Smac/DIABLO exists as a dimer, mediated by a hydrophobic interface within the N-termini of the individual molecules (Adrain, 2001).

Smac/DIABLO neutralizes inhibitor of Apoptosis proteins (IAPs), particularly interacting with the Baculovirus inhibitor of Apoptosis protein repeat (BIR) domains of X-linked inhibitor of apoptosis protein (XIAP). A particular NH_2- terminal motif, consisting of four amino acids (Alanine-Valine-Proline- Leucine) is responsible for the interaction with IAPs. This allows for the release of caspases -9 and -3 (Martinez-Ruiz, 2008). Martinez- Ruiz et al (2008) also stated that during cancer cell progression, lower Smac/DIABLO levels are seen and hence higher apoptosis resistance occurs (Martinez-Ruiz, 2008).

1.2.4.7 Oxidative stress in cancer and apoptosis:

Reactive oxygen species (ROS) are classified as oxygen-containing chemical species with reactive properties. The molecules are derived from oxygen used in metabolic reactions in the mitochondria, endoplasmic reticulum and the peroxisomes (Gorrini, 2013).

Cancer cell metabolism makes use of anaerobic glycolysis, which is termed as the Warburg effect (Heiden, 2009). This allows for the production of ROS from signal transduction and transcription factors (Gorrini, 2013, Noda, 2001). ROS and cell transformation in cancer cells were first established in 1981 and showed cancer cells to have a constant demand for ATP production and thus an accumulation of ROS which have different roles in the cell metabolism depending on the amount being produced (Gorrini, 2013).

ROS have very high chemical reactivity and affect cellular DNA, phospholipids, carbohydrates and proteins, resulting in protein oxidation and degradation as well as lipid peroxidation. Oxidative stress can lead to DNA damage by the modification of purine and pyrimidine bases leading to strand breaks. ROS react with DNA to form a range of cytotoxic oxidative base lesions, including 7, 8-dihydro-8-oxoguanine (8-oxoG). This oxidative base lesion is different from guanine as it pairs incorrectly with adenine, eventually leading to transversion mutations (Youn, 2007). Alterations in DNA sequences may alter and/or activate several proto-oncogenes and cause mutations in tumour suppressor genes such as p53 and cell-cycle related genes (Mátes, 2012, Noda, 2001). High levels of ROS generation in response to external stimuli lead to the activation of transcription factors which initiate apoptosis by caspases. ROS-induced DNA damage allows for the activation of p53 which allows for the modulation of programmed cell death and cell cycle arrest. Pro-apoptotic proteins Bax and Fas ligands allow for the initiation of apoptosis through sequential events leading to the activation of caspases. Bcl-2 is an anti-apoptotic protein which inhibits caspase activity and allows for cell survival (Figure 1.7).

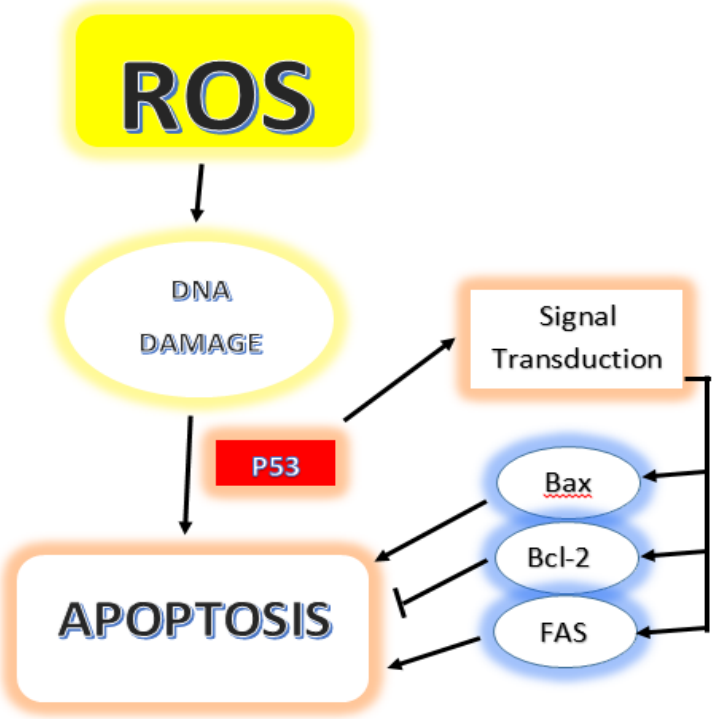

Figure 1.7: The induction of apoptosis due to ROS (Prepared by author).

1.2.4.7.1 Antioxidant response to Reactive Oxygen Species:

In normal cell metabolism, oxidizing equivalents in the form of ROS are generated during cellular respiration in the electron transport chain. Mitochondrial superoxide is the primary source of ROS produced. The formation of superoxide occurs due to the leak of electrons from the ETC at complexes I and II. Under normal conditions, complex IV reduces oxygen to form hydrogen peroxide, however, if a single electron is transferred to a dioxygen molecule at other points, superoxide may be formed, thus increasing oxidative stress levels (Jastroch, 2010). The cell's defence mechanism against increased oxidative stress is the production of antioxidants which act as reducing equivalents leading to a redox balance (Davis, 2000).

These antioxidants play a role in the removal of free radicals and protect the cell from oxidative damage (Valko, 2006). The transcription factor, nuclear factor erythroid 2 (Nrf2), which is found in the cytosol, is bound to Kelch-Like ECH- Associated Protein 1 (Keap 1) to form a complex keeping Nrf2 inactive. When ROS levels rise, oxidation of the cysteine residues binding Nrf2 to Keap1 facilitates the dissociation of Nrf2 from Keap1, allowing Nrf2 to translocate to the nucleus, where it exerts its activity. As seen in Figure 1.8, upon recognition of a consensus sequence, Nrf2 binds to the antioxidant response element (ARE), initiating the transcription of multiple antioxidant genes (Shih, 2005). Nrf2 is able to regulate the production of the endogenous antioxidant, reduced glutathione (GSH). In highly oxidative environments, hydrogen peroxide (H_2O_2) is able to oxidize GSH to glutathione disulphide (GSSG), thereby decreasing the ability of GSH as an antioxidant (Mátes, 2012).

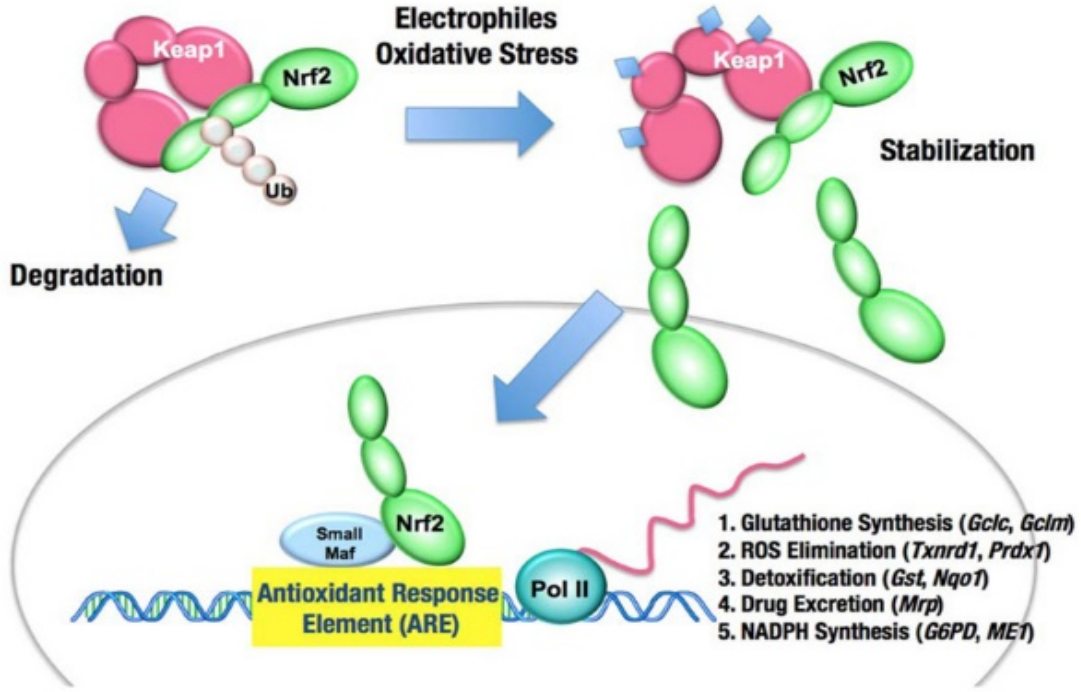

Figure 1.8: The Keap-Nrf 2 pathway- Regulation of antioxidant gene production by the activation and translocation of Nrf2 to the nucleus of the cell after dissociation from Keap1 (Mitsuishi, 2012).

1.2.4.8 The role of DNA Repair Enzymes PARP and OGG1 in Apoptosis:

Poly (ADP-ribose) polymerase-1 or PARP-1 catalyses the poly-ADP-ribosylation of specific nuclear proteins in order to repair DNA strand breaks and overall genomic maintenance. PARP-1 is the most abundant and well characterized enzyme of the PARP family. The enzyme consists of three conserved major domains, being, a NH_2 –terminal DNA-damage sensing and binding domain containing three zinc fingers, a C-terminal catalytic domain and an auto-modification domain. The zinc fingers play an important role in the activation of PARP1 with zinc 1 and 3 participating in the DNA-dependent activation of the enzyme.

When DNA breaks occur, as seen in Figure 1.9, PARP-1 is activated and cleaves nicotinamide adenine dinucleotide (NAD^+) to yield nicotinamide and ADP. The addition of ADP-ribose units together form a long branched chain attached to PARP-1, histones and other DNA repair proteins which form a polymer adjacent to the strand breaks. The polymer forms a scaffolding

and recruit other proteins that are critical to DNA repair including proteins involved in chromatin remodelling and chromosomal organisation (Javie, 2011).

In the late stages of Apoptosis, PARP1 is cleaved into 89 and 24 kDa fragment, thus inactivating the enzyme (Boulares, 2013, DÁmours, 2001). Javie *et al* (2011) discussed, in depth, the role of PARP inhibitors (PARPi) as chemotherapeutic agents. The cytotoxic agent contains analogues that are able to inhibit PARP1/2 and lead to the accumulation of damaged DNA, overwhelming alternative repair pathways and ultimately leading to cell death. Most PARPi are undergoing different phases of clinical trials (Javie, 2011).

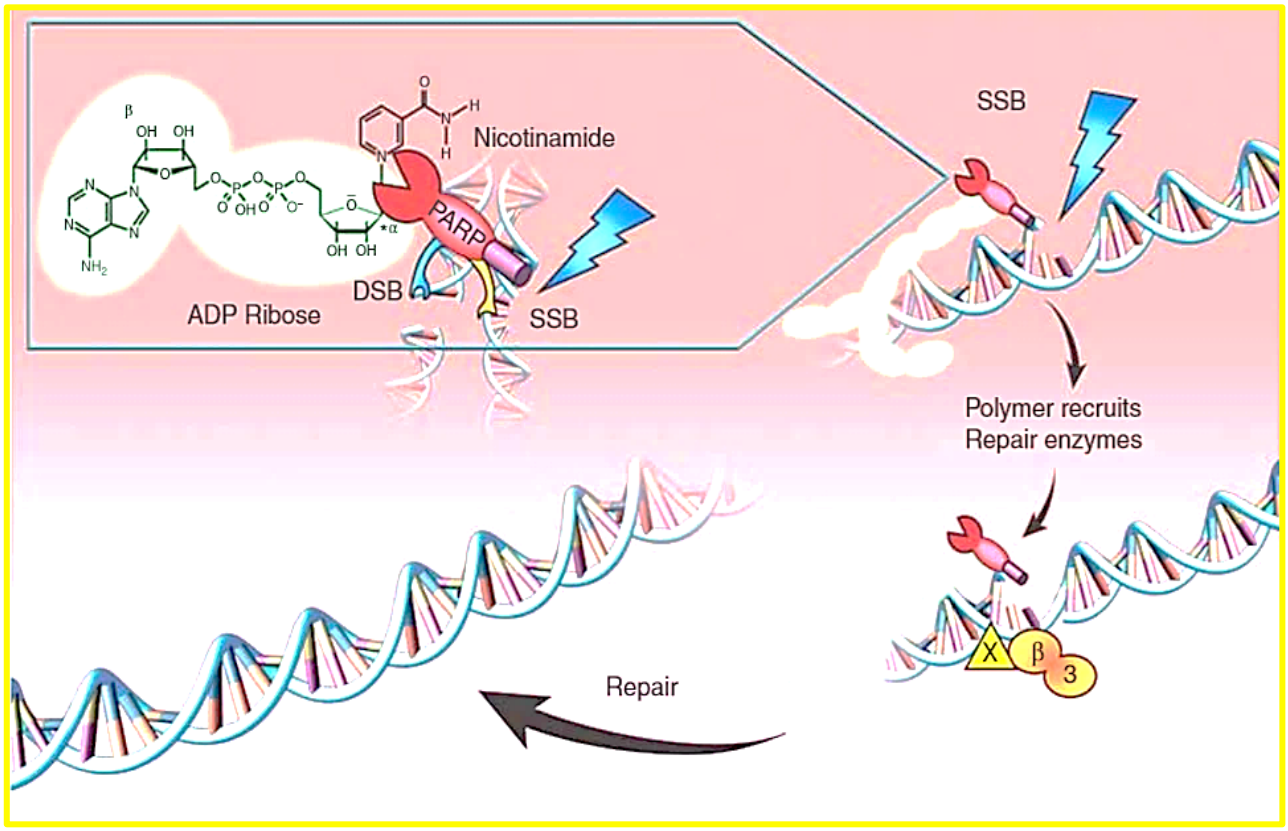

Figure 1.9: Catalytic activity of PARP-1. Cleavage of NAD^+ by PARP-1 allows for the formation of polymers which recruit and activate repair pathways for the single-stranded DNA breaks (SSB) (Javie, 2011).

Ineffective repair of damaged mitochondrial DNA due to oxidative stress may lead to mitochondrial dysfunction and apoptosis (Liu, 2011). 8–Oxoguanine glycosylase (*OGG1*) is a base excision repair enzyme which plays an important role in eukaryotes by allowing for repair to DNA in both the nuclear and mitochondrial genomes, thereby suppressing cell death (Youn, 2007). DNA base excision repair (BER) makes use of a four-step pathway (Figure 1.10). The

initial steps are the recognition of oxidative-damaged bases by *OGG1*, followed by the repair of the aberrant bases by Ape1/Ref1. *OGG1* has two enzymatic functions: glycosylase and lyase activity. The glycosylase activity cleaves the C1 glycosidic bond between the base and ribose sugar, this allows for the removal of the oxidized guanine and creates a vacant area next to cytosine, *OGG1* then nicks the phosphodiester backbone between the C3 bond of the ribose ring and the phosphate on the 3'side of the vacant area. This results in the single stranded break. Ape1 can then removes the residual ribose phosphate and produces 3'hydroxyl group (OH) which may be extended by DNA polymerase- β (McMurray, 2010). A new base is then inserted and the damaged strands are re-ligated by a DNA ligase (Liu, 2011).

Liu *et al* (2001) also stated that the overexpression of mitochondrial targeted *OGG1* prevents mitochondrial DNA damage and the intrinsic apoptotic pathway in vascular endothelial and asbestos-exposed cells (Liu, 2011). This suggests that the intrinsic apoptotic pathway may be regulated by *OGG1* during oxidative stress conditions.

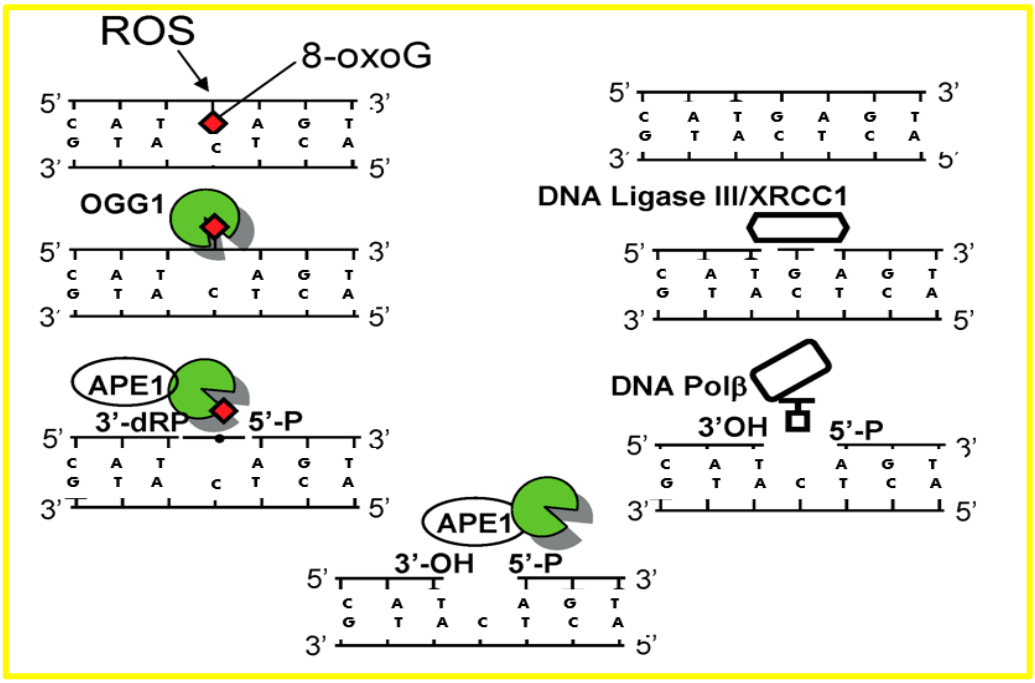

Figure 1.10: *OGG1* repair of 8-oxoG via DNA base excision repair pathway (BER) (adapted from (Ba, 2014)).

1.2.5 The Evasion of Apoptosis by Cancer Cells:

Cancer originates from a single cell. Carcinogenesis, the process in which a normal cell becomes a malignant cell, constitutes multiple complex molecular signalling pathways. The process of carcinogenesis may be defined by three processes i.e., initiation, promotion and

progression. Initiation occurs when a normal cell is transformed by gene mutations and altered metabolism to an initiated cell (Yokota, 2000). This altered metabolism exhibit different characteristics of normal cell metabolism, whereby, lactate is produced from glucose in aerobic conditions. This phenomenon was founded by Ota Warburg and is termed, the "Warburg'' effect (Cantor, 2012). Then, the initiated cell undergoes tumour promotion and turns into a pre-neoplastic cell, which subsequently develop to a neoplastic cell after progression stage (Yokota, 2000). The stage of promotion is characterized by uncontrollable cellular signalling pathways that manifest cell proliferation and alter programmed cell death (apoptosis).

Apoptosis is involved in the tissue homeostasis which may be characterized by the balance of proliferation versus cell death. Apoptotic dysregulation leads to cell survival and tumour growth (Fulda, 2006).

Malignant cells contain three major metabolic necessities:- ATP generation, increases in biosynthesis of macromolecules being carbohydrates, proteins, lipids and nucleic acids and lastly to alter intracellular reactive oxygen species (Cairns, 2011). Cancerous cells are able to alter and mutate key regulators of apoptosis, thereby maintaining survival and allowing for the proliferation of the cells (Figure 1.11).

In the extrinsic pathway, studies have shown that cancer cells have impaired death receptor surface expression as an adaptive cell response, this can be seen by a downregulation of CD95 expressed in neuroblastoma cells and colon carcinoma cells resistant to TRAIL-induced cell death (Fulda, 2006). Decoy receptors are also synthesized by cancer cells so that ligand binding cannot occur, hence the execution of apoptosis cannot occur. Cancer cells have also been shown to increase the expression of anti-apoptotic proteins Bcl-2 compared to that of pro-apoptotic proteins such as Bax and Bak. Studies show that these proteins are regulated by ROS production as Bcl-2 is localised to the mitochondrial membrane, nuclear envelope and ER. Cytochrome C regulates apoptosis when oxidized cytochrome C induces apoptosis and the reduced form of the molecule inhibits the programmed cell death (Wong, 2011, Fulda, 2006). Tumour resistance to apoptosis may also be caused due to aberrant IAPs. The translation of XIAP and cIAP1 are via internal ribosome entry sites (IRES) which allows for translation of the proteins even under stress conditions when protein synthesis is usually shut down (Fulda, 2009). Fulda (2009) also stated that IRES-mediated translational regulation of XIAP and cIAP1 enables a rapid response to transient cellular stress conditions in order to delay cell death and ensure survival of the cell (Fulda, 2009).

Cell proliferation in normal cells is a highly regulated process controlled by checkpoints and proteins of the cell cycle. The G_0 /resting phase of the cell cycle is important as antigrowth

signals exert their influence to block cell proliferation in aberrant cycles. Most cancer cells are able to evade this checkpoint and inhibit normal growth suppression in order to continue proliferation. The two tumour suppressors most commonly mutated in cancer cells are P53 and retinoblastoma protein. Retinoblastoma (Rb) is found at a checkpoint at the G_1 phase whereby it restricts cell passage to the next phase. Cells with mutated Rb inhibit this regulation and allow ongoing cell proliferation (Collard, 2012). P53 acts as a central regulator of apoptosis and arrests cell cycle due to DNA damage. Aberrant p53 allows the progression of the cell cycle despite DNA damage and cellular stresses (Fridman, 2003).

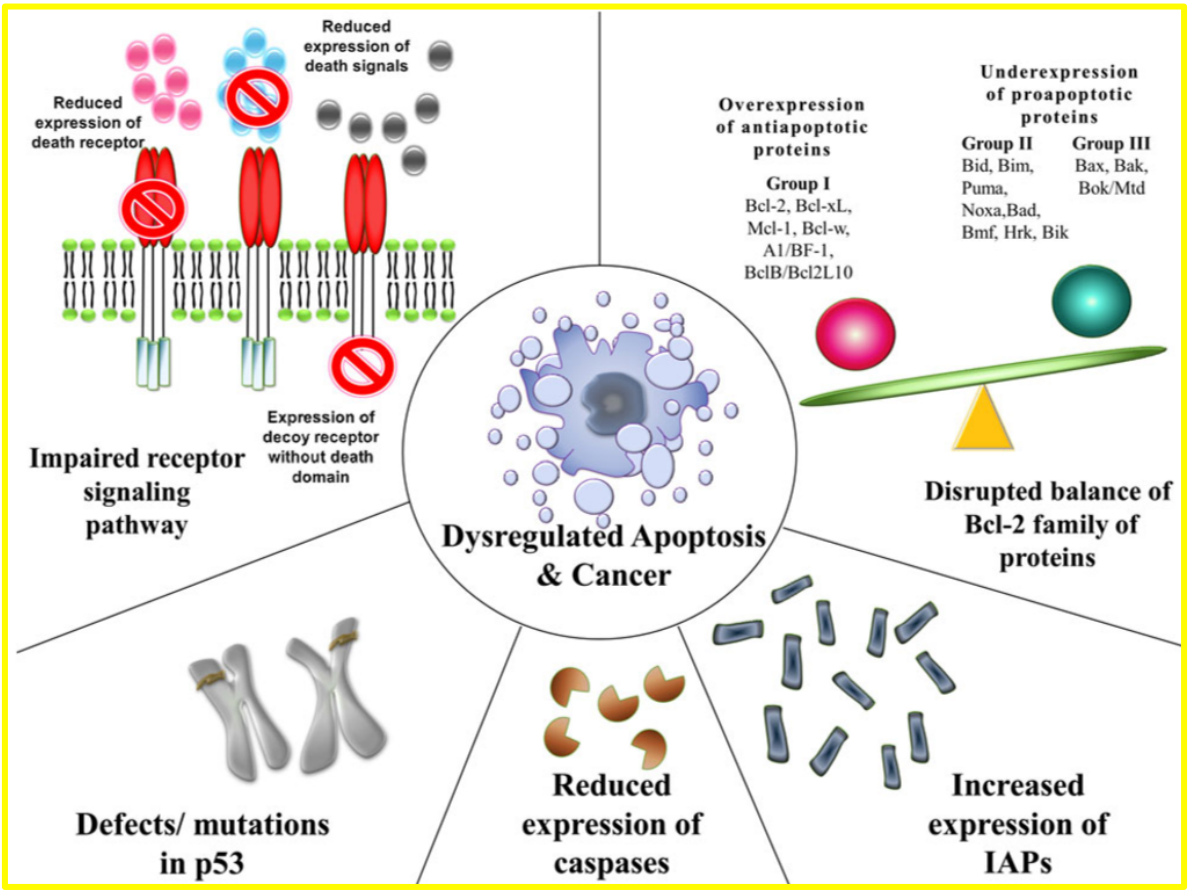

Figure 1.11: Schematic of Evasion of Apoptosis by cancer cells (Wong, 2011).

1.3 AIM AND OBJECTIVES

Hypothesis:

It may be hypothesized that ATO does not have any effect on human lung adenocarcinoma cells (A549).

Aim:

To determine the cytotoxic effects of ATO on human lung adenocarcinoma cells (A549) by investigating molecular events contributing to cell death following acute exposure after 48 hours.

The objectives of the study were to determine:

- The effect of ATO on cell viability and respiratory output in human lung carcinoma A549 cell viability using the MTT assay.
- The oxidative status of A549 cells exposed to ATO by quantification of the biomarker of malondialdehyde (MDA) using the TBARS assay, and to assess the endogenous antioxidant response (glutathione and Nrf2).
- The apoptotic pathways induced using ATO by luminometric quantification of caspase (8/9/3/7) activity, and protein expression of apoptotic markers (BCl2, Bax, p53, SMAC/DIABLO) via western blot.
- DNA integrity following ATO administration in A549 cells by assessing DNA fragmentation via the comet (SCGE) assay, DNA repair enzymes PARP-1 and *OGG1*, and nuclear morphological features of apoptosis using Hoechst assay.

CHAPTER 2-
MATERIALS AND METHODS

2.1 Materials:

The A549 cells were purchased from Highveld Biologicals (Johannesburg, SA). Cell culture reagents were purchased from Whitehead Scientific (Johannesburg, SA). Western blot reagents were purchased from Bio-Rad (Hercules, CA, USA). CellTitre Glo GSH-Glo Caspase -8, -9 and -3/7 Glo luminometry assays were purchased from Promega. All other reagents and consumables were purchased from Merck (SA), unless stated otherwise.

2.2 Atorvastatin Preparation:

A 1mg/ml stock solution was prepared by dissolving 2 x Aspavor20 (20mg Atorvastatin) tablets (A39/7.5/0018- Pfizer, Johnnesburg, SA) in 40ml of 0.1M phosphate-buffered saline (PBS). Subsequent treatments were diluted from stored stock solution (4°C).

2.3 Cell Culture and Exposure Protocol:

The A549 cells were cultured (37°C, 5%, CO_2) in complete culture media (CCM) [Eagle's minimum essential medium supplemented with 1% L-glutamine, 1% penstrepfungizone and 10% foetal bovine serum]. Following the determination of the concentration of half maximum inhibition (IC_{50}), all treatments for subsequent assays, with the exception of the MTT assay, were conducted in $25cm^3$ sterile cell culture flasks for a duration of 48 hours (h).

2.4 MTT Assay:

2.4.1 Introduction-

Methylthiazol tetrazolium is a yellow water-soluble tetrazolium dye, that when reduced by viable cells turns into a purple water insoluble formazan product. This technique is useful for cells that are metabolically active based on their redox potential and capacity of dehydrogenase

enzymes to convert yellow water-soluble salt into the formazan product, thus the colour function is a useful marker of only viable cells (Figure 2.1). The reaction depends on enzymes that catalyse the transfer of electrons to an oxidant compound. The tricarboxylic acid (TCA) cycle contains molecules such as NADH/ NADPH/ FADH which are oxidized to NAD^+/ $NADP^+$/ FAD^+ by oxidoreductases (Oka, 1992, Riss, 2013).

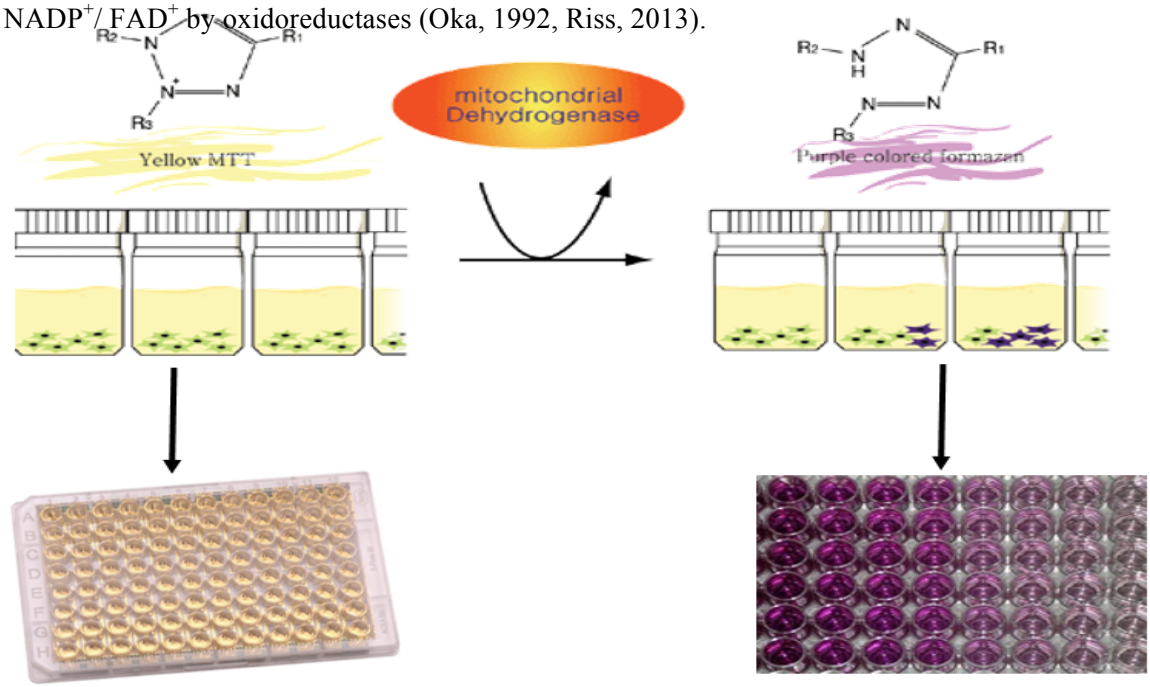

Figure 2.1: Reduction of MTT salt to formazan by viable cells (Adapted from http://www.sakeenagilani/mtt-assay-for-cell-viability).

2.4.2 Protocol-

The cytotoxicity of ATO in A549 cells was measured by the MTT assay. Cells (15,000 cells/well) in 4 replicates were seeded in a 96-well microtitre plate and allowed to attach overnight (37°C, 5% CO_2). Cells were then subject to treatment with a range of ATO concentrations (0-150µg/ml). Following a 48h incubation, the cells were incubated (37°C, 4h) with MTT substrate (5mg/ml in 0.1M PBS). Thereafter, supernatants were aspirated and cells were incubated in dimethyl sulphoxide (DMSO; 100µl/well) for 1 h. Optical density (OD) was then measured at 570nm, with a reference wavelength of 690nm by an enzyme-linked immunosorbent assay (ELISA) plate reader (Bio Tek µQuant, USA). The percentage cell viability was calculated by utilising the equation below and a concentration- response curve was plotted using GraphPad Prism V5.0 software (USA). Each experiment was conducted twice on separate occasions in order to confirm the data results from the first set matched the repeated experiment. The IC_{50} was calculated. For subsequent assays, A549 cells were treated at 80% confluency with an IC_{50} of 39.25µg/ml for 48 h.

% Cell viability = $\frac{\text{mean absorbance of treated cells}}{\text{mean absorbance of control cells}}$ x 100

2.5 ATP Assay:

2.5.1 Introduction-

ATP is a complex nano-machine that serves as the primary energy currency of the cell and is the most widely distributed high-energy compound within the human body, thus its production is essential for living organisms. The mitochondria is known as the cell's "power house," where cellular energy is produced in the form of ATP.

ATP may be produced via glycolysis or cellular respiration, there are three subways pyruvate oxidation, the tricarboxylic acid (TCA) cycle and the electron transport chain (Figure 2.2). The highest amount of ATP is produced in the electron transport chain via oxidative phosphorylation (Bergman, 2015, Riss, 2013).

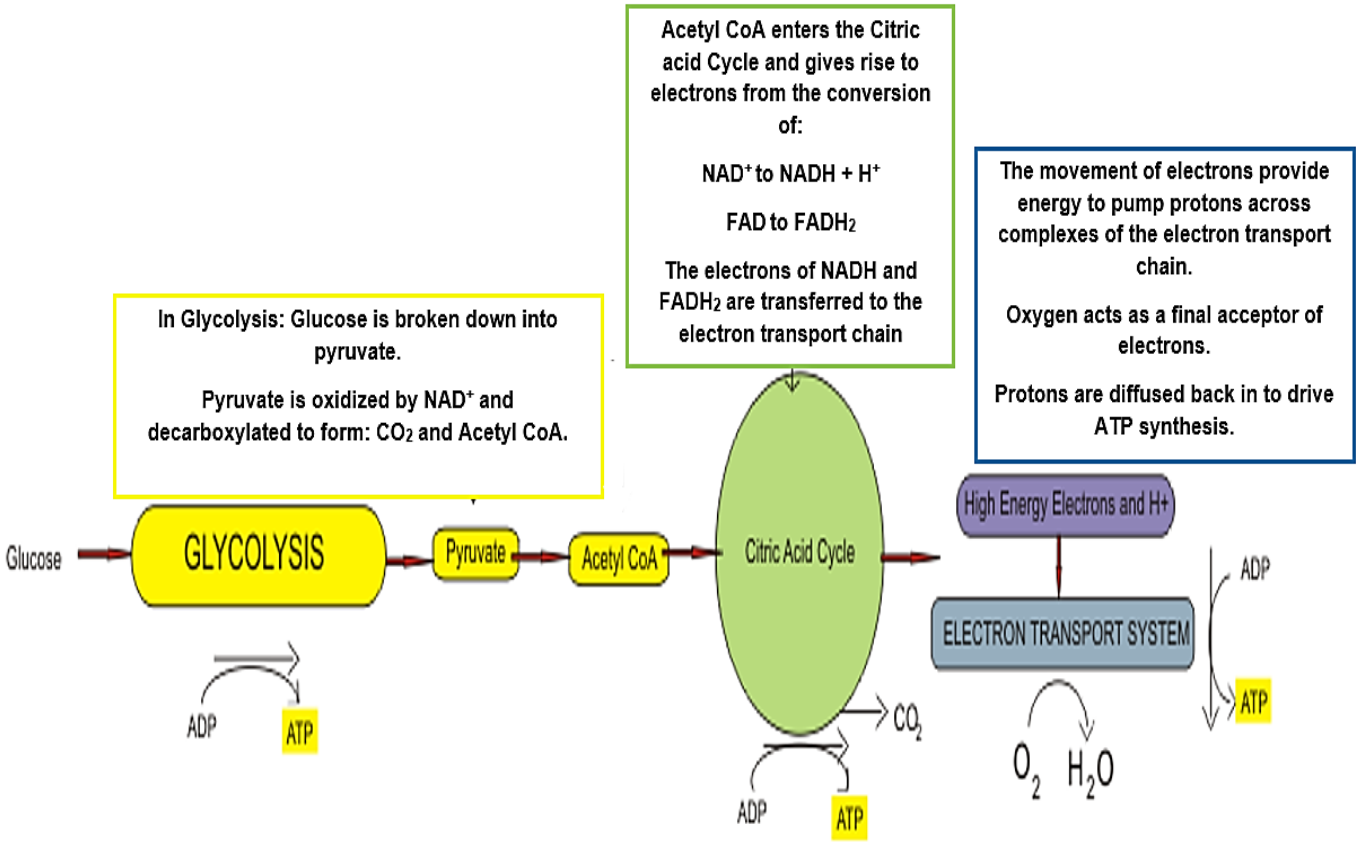

Figure 2.2: Schematic representation of glycolysis, TCA cycle and the electron transport chain. All pathways converge and cofactors are transported from one pathway to the other to allow for optimum ATP production (Adapted from https://en.m.wikibooks.org/wiki/Medical_Physiology/Basic_Biochemistry/Sugars).

2.5.2 Protocol-

Adenosine triphosphate (ATP) was measured by the luminometric Cell Titer-Glo® assay (G775A, Promega, Madison, Wisconsin, USA). The assay was independently conducted twice. The ATP quantification assay utilises bioluminescence to ascertain ATP levels in cells. The assay is based on the conversion of a luciferase-inactive derivative by ATP in the presence of magnesium ions to D-luciferin. D-luciferin, a luciferase substrate, reacts with the enzyme luciferase to produce oxyluciferin and release energy in the form of luminescence (Figure 2.3). This luminescent signal is directly proportional to the concentration of ATP present in the cells. Cells were seeded in triplicate in a white microtitre plate (20,000 cells per well) in a 1:2 ratio with ATP Cell Titer-Glo Reagent. The plate was incubated for 30-min at RT. Luminescence was measured on a Modulus™ microplate luminometer (Turner BioSystems, Sunnyvale, California, USA). Luminescence is proportional to ATP concentration and was expressed as relative light units (RLU).

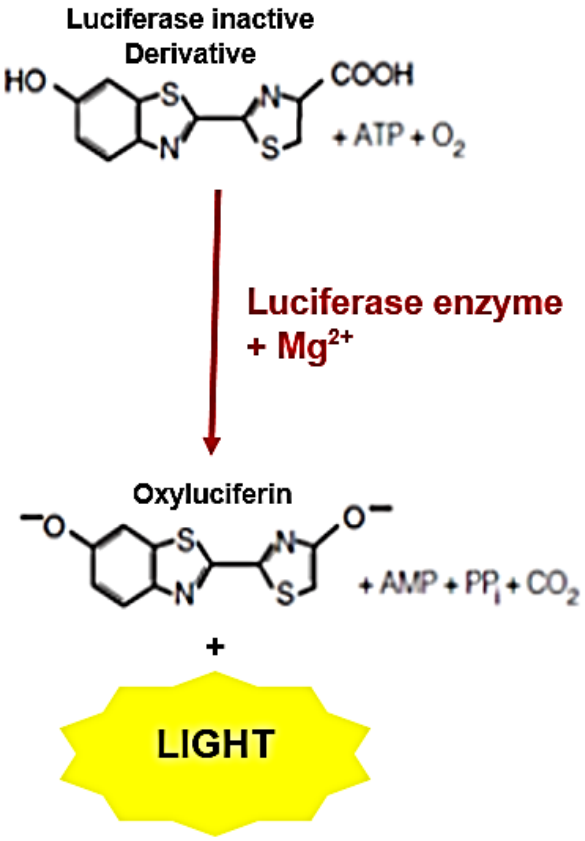

Figure 2.3: The luciferase reaction in the presence of magnesium, ATP and molecular oxygen (Adapted from (Govender, 2012)).

2.6 Lactate Dehydrogenase (LDH) Assay:

2.6.1 Introduction-

Lactate dehydrogenase is a cytoplasmic enzyme that is found in all major organ systems. In the final step of anaerobic glycolysis, the enzyme allows for the transfer of hydrogen, which catalyzes the oxidation of L-Lactate to pyruvate with nicotinamide-adenine dinucleotide (NAD^+) as the hydrogen acceptor. The reaction is reversible, but favours the reverse reaction of pyruvate to lactate. Activity of LDH is present in almost all cells of the body and is an exclusively cytosolic enzyme. During cell damage, LDH leaks out of the compromised cell membrane into the extracellular space (Figure 2.4), thus extracellular LDH levels are a marker of cell death or damage due to a wide range of factors including ischaemia, dehydration and exposure to toxins or chemicals (Drent, 1996).

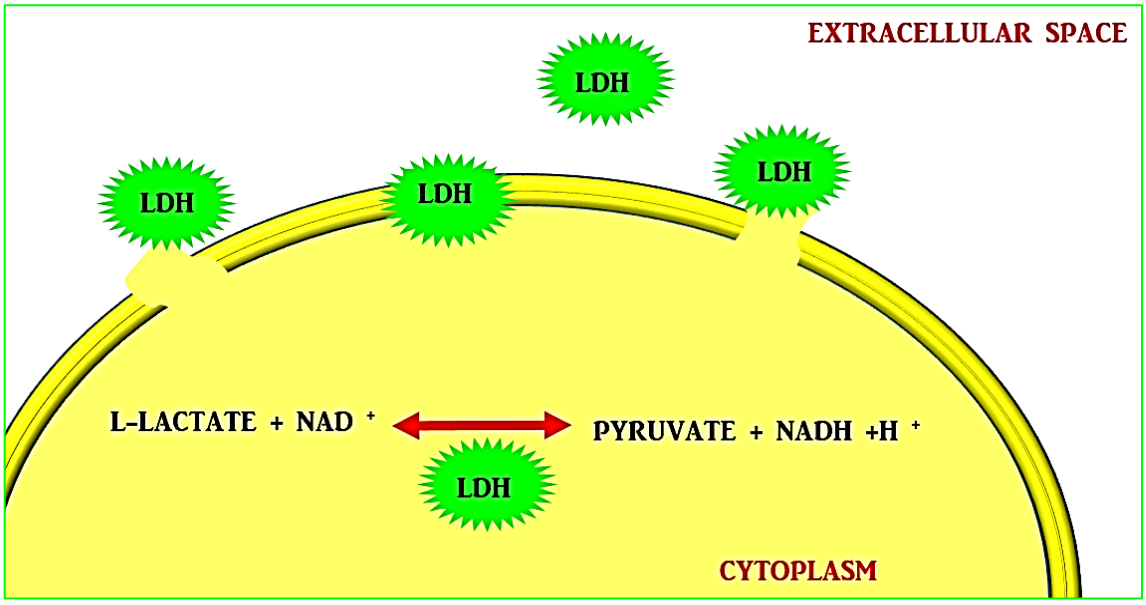

Figure 2.4: Schematic representation of compromised cell membrane. Lactate Dehydrogenase which is primarily found in the cytoplasm leaks into extracellular space during cell damage (Prepared by Author).

2.6.2 Protocol-

The LDH cytotoxicity detection kit (Roche, Mannheim, Germany) was used to measure cell death/damage of ATO treated A549 cells. A colorimetric assay was conducted twice on separate

occasions for the quantification of LDH activity in the supernatant of samples. The assay is a two-step enzymatic reaction where NAD^+ is reduced to $NADH/H^+$ by the conversion of lactate to pyruvate. Thereafter, a diaphorase catalyst transfers H/H^+ from $NADH/H^+$ to a tetrazolium salt to yield a formazan product. To measure LDH activity, supernatant (100µl) was transferred, in triplicate, into a microtitre plate in triplicate. Thereafter, substrate mixture (100µl) containing catalyst (diaphorase/NAD^+) and dye solution (INT/sodium lactate) from the kit was added to the supernatant and allowed to react at ambient temperature for 25 minutes. Optical density of the resulting formazan product was measured at 500nm with an ELISA plate reader (Bio-Tek uQuant). Results are represented as mean optical density.

2.7 Glutathione Assay:

2.7.1 Introduction-

When there are increased reactive oxygen species in cells, endogenous antioxidants counteract the effects of oxidative stress. Glutathione (GSH) is the one of the most powerful antioxidant and detoxifying agents in all human cells due to its protective abilities against radical damage. It is a small protein molecule composed of three amino acids: cysteine, glutamate and glycine, called GSH precursors or building blocks. The anti-oxidant tripeptide plays an important role in the detoxification of peroxides and electrophilic species. Glutathione exists both in a reduced (GSH) and oxidized (GSSG) state. The thiol group of cysteine is able to donate a reducing equivalent, catalysed by glutathione peroxidase, to detoxify peroxides. Peroxynitrite, hydroxyl radical and lipid peroxy-radicals are also detoxified by glutathione. When an electron is donated, GSH is oxidized to GSSG which is more reactive. GSH can be regenerated from GSSG by the enzyme glutathione reductase (Powers, 2008). NADPH and FAD act as cofactors in the reaction, as illustrated below (Figure 2.5):

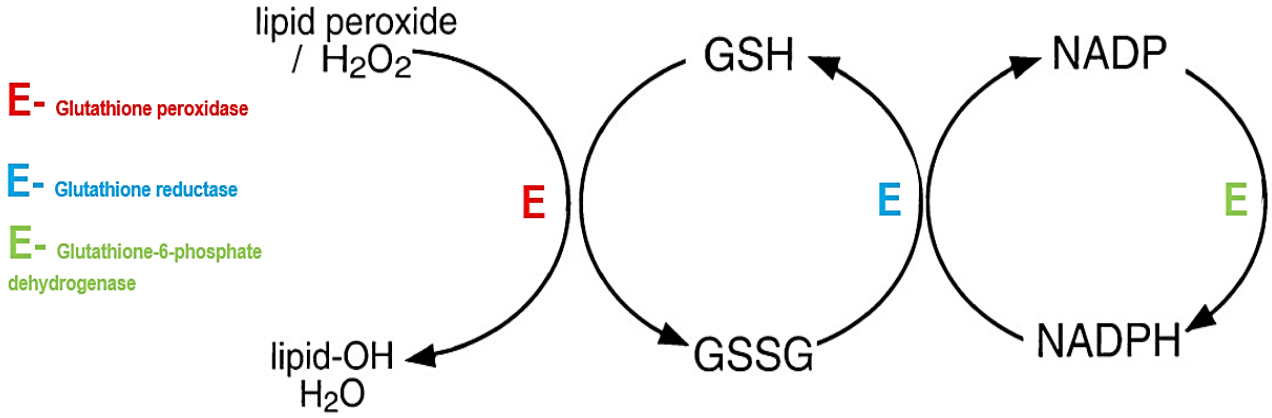

Figure 2.5: Detoxification of H_2O_2 by glutathione-S-transferase and the regeneration of glutathione from glutathione disulphide by glutathione reductase (Adapted from (Rahman, 1999)).

2.7.2 Protocol:

The GSH-Glo™ Glutathione assay (V6911, Promega) was utilized to quantify intracellular GSH levels. Subsequent to treatment of cells, 20 000 cells/well were added in triplicate in an opaque 96-well microtitre plate and 50µl of 1X GSH-Glo™ reagent (prepared according to manufacturer's guidelines) was added. GSH standards (0-25µM) were serially diluted (two-fold) from a 5mM stock in de-ionised water. After 30min incubation at RT, 50µl of luciferin detection reagent was added to the wells (15min, RT). Luminescence was detected on a Modulus™ microplate luminometer. A standard curve was constructed and sample GSH concentrations (µM) were calculated.

2.8 Lipid Peroxidation:

2.8.1 Introduction-

Lipid peroxidation can be defined as the oxidative deterioration of lipids containing any number of carbon- carbon double bonds. In response to membrane lipid peroxidation, cells may either promote cell survival or induce cell death. The overall process of lipid peroxidation consists of three steps: initiation, propagation and termination. Once lipid peroxidation is initiated, a propagation of chain reactions will take place until termination products are produced. Lipid peroxidation or reaction of oxygen with unsaturated lipid produces a wide variety of oxidation products including Malondialdehyde (MDA), which may be used as a reliable marker for oxidative stress (Mylonas, 1999).

2.8.2 Protocol:

Oxidative damage by ATO on A549 lung cells were assessed by the Thiobarbituric acid assay (TBARS). TBARS measures Malondialdehyde (MDA) which is the by-product of lipid peroxidation in cells. Following 48h treatment with ATO, cell culture supernatant (400µl) was dispensed, in duplicate, into glass tubes, with the addition of 2% phosphoric acid (200µl), 7% phosphoric acid (400µl) and TBA/BHT solution (400µl). A positive control of MDA and a negative control (400ul 3mM HCl) were prepared. All samples were adjusted to pH 1.5 and boiled for 15min to allow for the reaction depicted in Figure 2.6 to occur. Once cooled, butanol (1,5ml) was added to each test tube, vortexed and allowed to separate into distinct phases. The upper phase (800µl) was transferred into and centrifuged (840 x *g*, 6min, RT). 100µl from each

sample was aliquot into a 96-well microtitre plate in triplicate. The optical density was measured on a spectrophotometer at 532nm with reference wavelength of 600nm (Bio-Tek μQuant, USA). The assay was completed on three separate occasions to validate the obtained results. The sample means were calculated and divided by the absorption coefficient, $156mM^{-1}$ to yield the mean MDA concentration (μM).

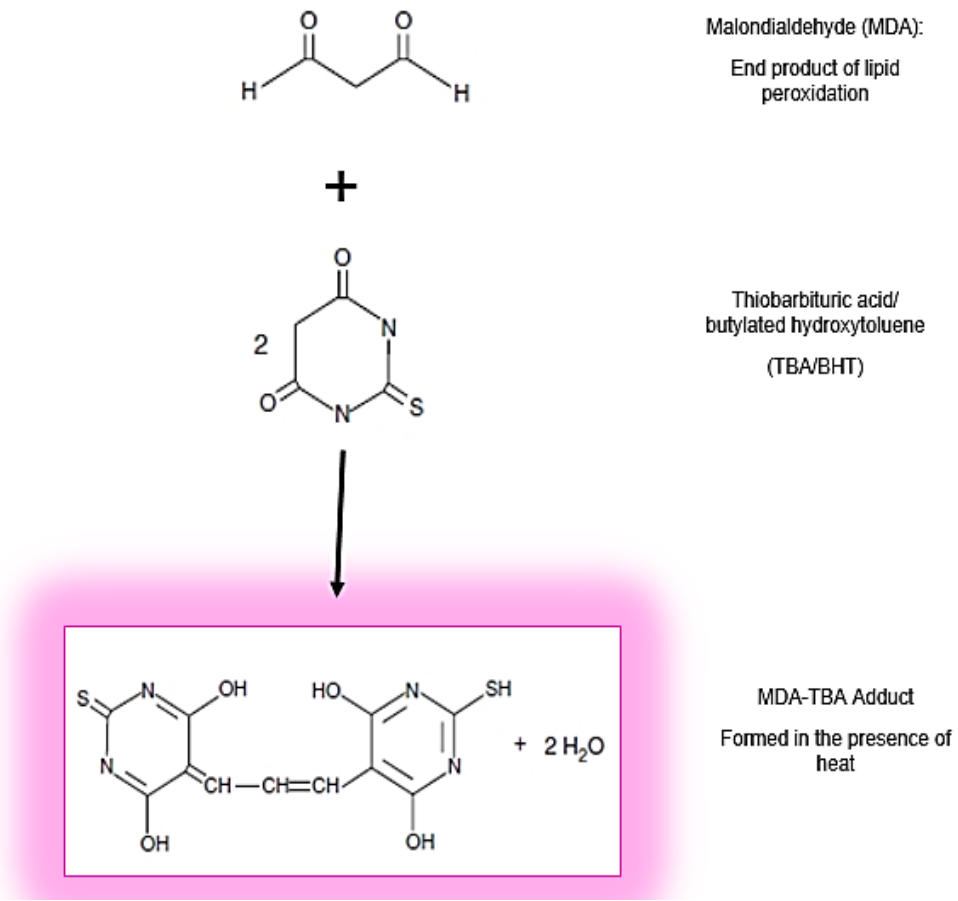

Figure 2.6: Schematic of TBARS assay overall reaction (Adapted from http://www.biotek.com/resources/articles/reactive-oxygen-species.html).

2.9 Caspase Activity:

2.9.1 Introduction-

Caspases are a family of cysteine proteases that play a crucial role in apoptosis as they are responsible for executing programmed cell death. Caspases 8 and 9 are initiator caspases and exist as inactive zymogens that are activated by dimerization. These initiator caspases activate

caspase 3/7 by cleavage of the procaspase. Once activated, one executioner caspase can cleave and activate other executioner caspases leading to an increased feedback loop of caspase activation (Brentnall, 2013). The luminometric caspase activity assay is used to determine the activity of caspases by the cleavage of caspase-specific luciferin substrate. The amount of light generated by luciferase is therefore proportional to the activity of the caspase (Figure 2.7).

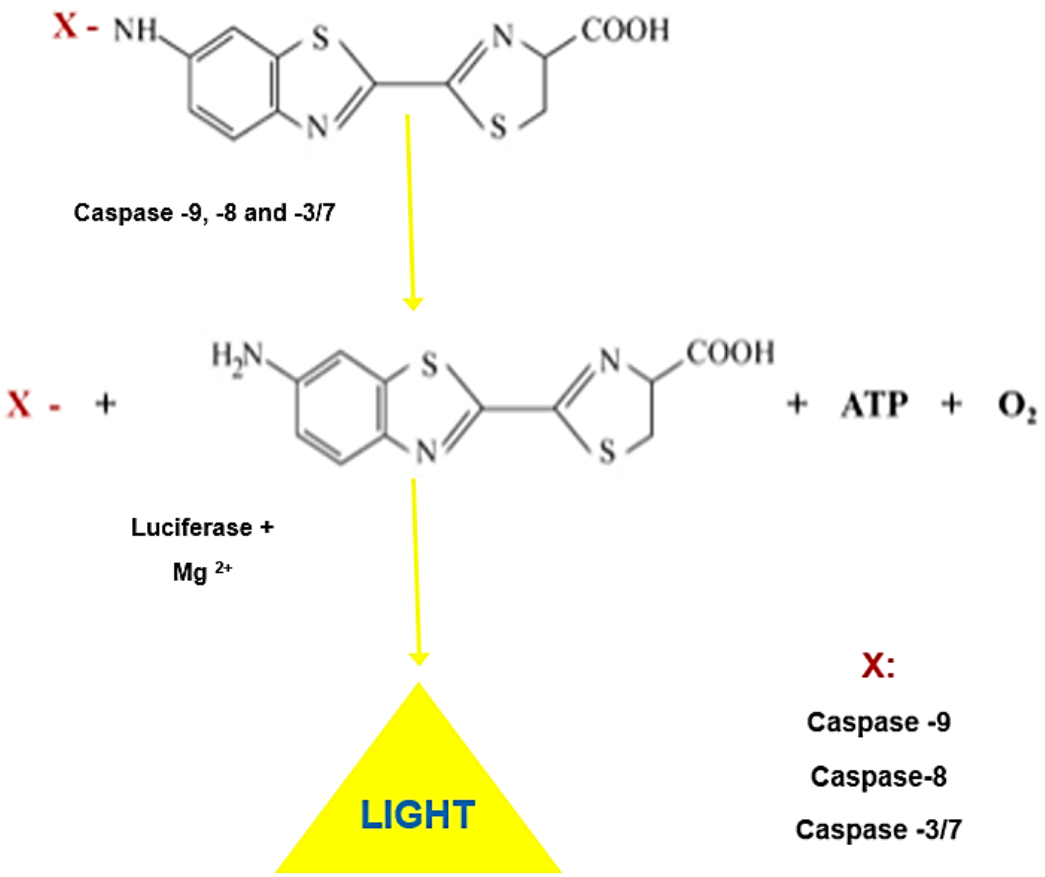

Figure 2.7 : Luminometric caspase activity assay depicting the reaction principle (Adapted from (Govender, 2012)).

2.9.2 Protocol-

Caspase-Glo® 3/ 7 (G8092), Caspase-Glo® 8 (G88201) and Caspase-Glo® 9 (CG8211) were used to assess apoptosis (Promega, Madison, USA). Reagents were prepared according to manufacturer's guidelines. A549 cells were added to wells (three replicates) of a white 96-well microtitre plate (20,000 cells in 150 µl CCM/well). Caspase reagent (100µl) were added and

incubated in the dark (30min, RT). The luminescent signal was measured on a Modulus™ microplate luminometer. The assay was conducted on three separate occasions to confirm the data results. Caspase-3/-7, -8 and -9 activities were expressed as relative light units (RLU).

2.10 Comet Assay:

2.10.1 Introduction-

Single cell gel electrophoresis (SCGE), otherwise known as the comet assay, is a procedure that is able to detect DNA strand breaks due to genotoxic stimuli. The fragmentation of DNA is a late apoptotic feature and is mediated by a group of proteins that are released downstream of the apoptotic cascade. The 'comet' refers to the appearance of the DNA from an individual cell following electrophoretic migration (Figure 2.8). The comet head contains high molecular weight DNA and the comet tail contains the leading ends of migrating fragments. The comet assay combines DNA gel electrophoresis with fluorescence microscopy to visualize migration of DNA strands from individual agarose-embedded cells (Olive, 2006).

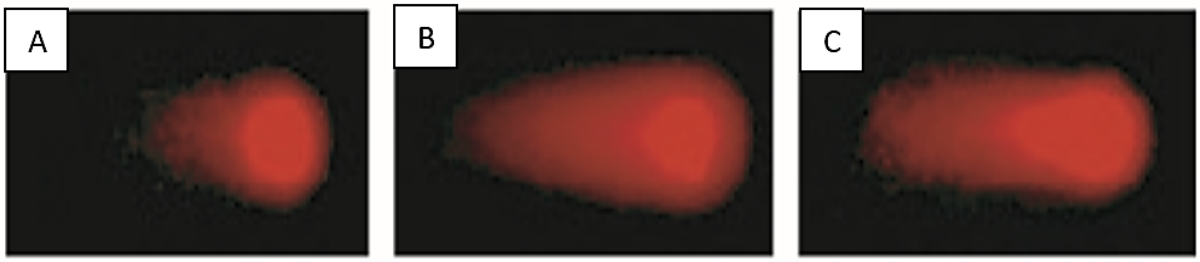

Figure 2.8: Comet formation after electrophoresis (Olive, 2006). Negatively charged DNA contain breaks, DNA supercoils are relaxed and broken ends are able to migrate toward anode during electrophoresis (Figures **B** and **C**). If the DNA is undamaged the lack of free ends and the large size of the fragments prevent migration during electrophoresis (Figure **A**). Cancer cells however, will have some degree of DNA fragmentation due to mutations and alterations of genomic molecules.

2.10.2 Protocol-

The comet assay was used to determine DNA fragmentation in treated cells. Briefly, three frosted end microscope slides were prepared for both control and treatment, a first layer containing 400µl of 1% low melting point agarose (LMPA, 37°C) which were incubated at 4°C for 10 minutes, a second layer of 25µl of cell suspension (20,000 cells suspended in 0.1M PBS) from each sample with 175µl 0.5% LMPA (37°C), and 1µl GR Red (fluorescent staining dye) which was allowed to solidify for 10 minutes at 4°C. A third layer containing 200µl of 1%

LMPA (37°C) was then added and allowed to incubate for approximately 10minutes at 4°C. Cover slips were removed and slides were subjected to lysis (4°C, 1hr, protected from light) by being submerged in cell lysis buffer (2.5M NaCl, 100mM EDTA, 1% Triton X-100, 10mM Tris (pH 10) and 10% DMSO). The slides were equilibrated in electrophoresis buffer (300mM NaOH, 1mM Na_2EDTA, pH 13; 20min) then electrophoresed (300mA, 25V, 35min) after which slides were washed three times (0.4M Tris, pH 7.4; 5min). Cover slips were placed onto slides and maintained overnight at 4°C. Slides were viewed using a fluorescent microscope (Olympus IXSI inverted microscope/510-560nm excitation and 590nm emission wavelengths). Images were captured and comet tails of 50 cells were measured using Life Science-Soft Imaging System (analySIS® v5). The assay was conducted on two separate occasions for confirmation of the first data set. The results were expressed as mean tail length in µm.

2.11 Hoechst Stain Assay:

2.11.1 Introduction-

Hoechst is a water-soluble blue fluorescent, photosensitive dye, which is positive under physiological conditions. Hoechst 33342 is able to permeate viable cell membranes and stain double stranded nuclear DNA, thereby allowing the visualization and identification of replicating or apoptotic cells. Hoechst 33342 binds to the minor groove of the double helix, preferentially to Adenosine-Thymine rich regions (Figure 2.9). Hoechst excites at λ = 350nm and emits at λ = 461nm. Fluorescent microscopy is used to view the stained cells. The Hoechst stain is used to visualize the effect of a compound on DNA, apoptotic studies and for cell cycle analysis (Vekshin, 2011).

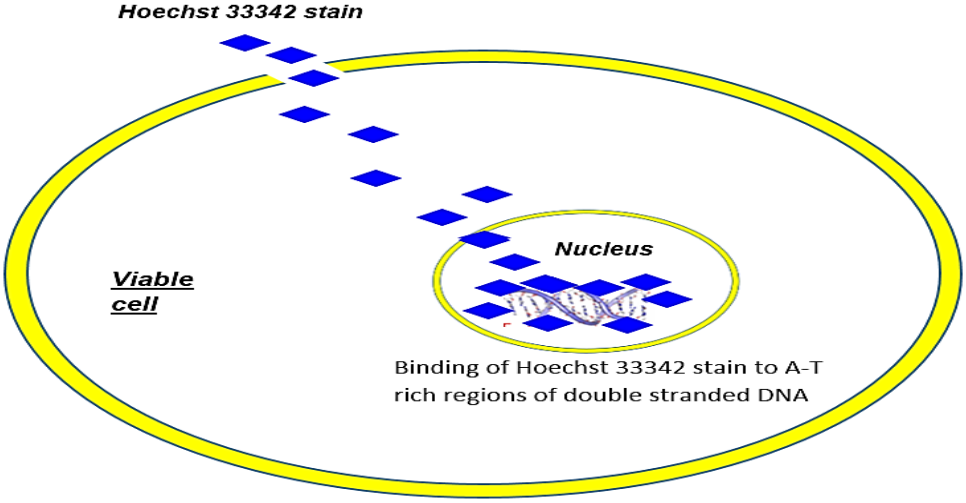

Figure 2.9: Nuclear staining with Hoechst 33342 in metabolically active cells (Prepared by Author).

2.11.2 Protocol-

To assess the effect of ATO on nuclear material, cells were stained with Hoescht 33342. Cells seeded at a density of 500,000 cells/well in a 6 well plate were treated in 3 replicates for 48h. Cells were washed 3 times with 0.1M PBS and fixed with 10% paraformaldehyde for 5min. Cells were washed with 0.1M PBS before Hoescht working solution was added (10µg/ml, Molecular probes, Eugene, OR). Following 15min incubation at 37°C, cells were prepared for microscopy. Images were captured with an Olympus IXSI inverted microscope using 350nm excitation and 450nm emission filters. Three images per treatment replicate were captured at 20x and 40x magnification.

2.12 Western Blot:

2.12.1 Protein Preparation-

Cytobuster™ reagent (Novagen) supplemented with protease and phosphatase inhibitors (Roche, 05892791001 and 04906837001 respectively) was used for protein isolation. Cytobuster (200µl) was added to the cells (4°C, 10min) and centrifuged (180-x-g; 4°C, 10min) to obtain a crude protein extract.

Following the isolation of protein from cells, crude extracts were quantified and standardised using the bicinchoninic acid (BCA) assay. The principle of the BCA assay is based on the Biuret reaction. The Biuret reaction measures the conversion of Cu^{2+} to Cu^{+}. In alkaline conditions Cu^{2+} reacts with peptide bonds to form Cu^{+}, which then reacts with BCA to produce an intense violet product at 37°C. BCA and copper interact with cysteine, tryptophan and tyrosine residues which lead to the colour development (Smith, 1985). It is necessary to quantify protein samples in order to know the concentration of protein within the sample. Protein standards (0; 0.2; 0.4; 0.6; 0.8, 1mg/ml) were made up using bovine serum albumin (BSA).The plate was then incubated for 1 hr at 37°C. Absorbance was read on the µQuant BioTek ELISA plate reader (λ = 562nm). The absorbance from the standards was used to construct a standard curve to calculate protein concentrations of the sample which were standardized to 0.8 mg/ml in Cytobuster. Standardisation prior to electrophoresis is important because it is necessary to have the same volume and concentration of sample in each well in order to measure the behaviour of the sample throughout the assay.

Following protein standardisation, samples are prepared with sample buffer containing SDS, tracker dye-bromophenol blue, glycerol and β-mercaptoethanol. Sodium dodecyl sulphate is an anionic detergent which is able to denature proteins by forming micelles around the

polypeptide. This gives the protein a negative charge and will be able to migrate in an electric field through the gel toward a positive electrode. Bromophenol blue is used as a tracking dye to monitor the migration of the proteins during electrophoresis, β-mercaptoethanol breaks inter and intra-molecular disulfide bonds to accommodate proper separation of the bands according to size and glycerol adds density to the sample to allow for sinking of the sample to the bottom of the well, decreasing the chance of dissemination of samples between wells.

Samples were then denatured by boiling for 15min with a 4:1 dilution of 5 x Laemmli sample buffer [0.375 Tris-HCL pH 6.8;10% w/v SDS; 3% v/v glycerol; 2% w/v bromophenol blue; 12% β-mercaptoethanol in dH_2O] to activate SDS .

2.12.2 Electrophoresis and Transfer-

After samples were prepared, they were separated by size using Sodium dodecyl sulphate polyacrylamide gel electrophoresis (SDS-PAGE). SDS-PAGE gels consist of a resolving gel, which is poured between two glass plates and topped by a short stacking gel. A lower percentage of acrylamide is used to improve transfer results. A 10% SDS-polyacrylamide resolving gel and a 4% stacking gel was prepared (dH2O, Tris, SDS, Bis/Acrylamide, 10% Ammonium phosphate sulphide, TEMED). TEMED is able to initiate Bis-acrylamide which acts as a cross linking agent, facilitating polymerization of the acrylamide gel. The cross-linked matrix formed by the polymerized acrylamide creates a porous structure through which the proteins will migrate. The migration allows for the separation proteins by molecular weight, with smaller proteins migrating further than larger proteins through the polyacrylamide matrix. . This makes it possible to clearly identify the target protein later through immunodetection with specific antibodies. Samples were loaded on the gel and electrophoresed at 150V for 1h.

Thereafter, protein bands are transferred from the gel to a nitrocellulose membrane via a wet transfer method as explained by Mahmood and Yang (Mahmood, 2012). This is a sandwich of – gel, nitrocellulose membrane and fibre pads, placed in cassette and immersed in a buffer tank which is subjected to an electric field (Figure 2.10). Transfer to nitrocellulose membranes was conducted at 400mA for 1h.The application of a current allows for the transfer from the gel to the membrane. The wet transfer is considered more reliable because it is less likely to dry out the gel and the membrane (Mahmood, 2012, Taylor, 2014).

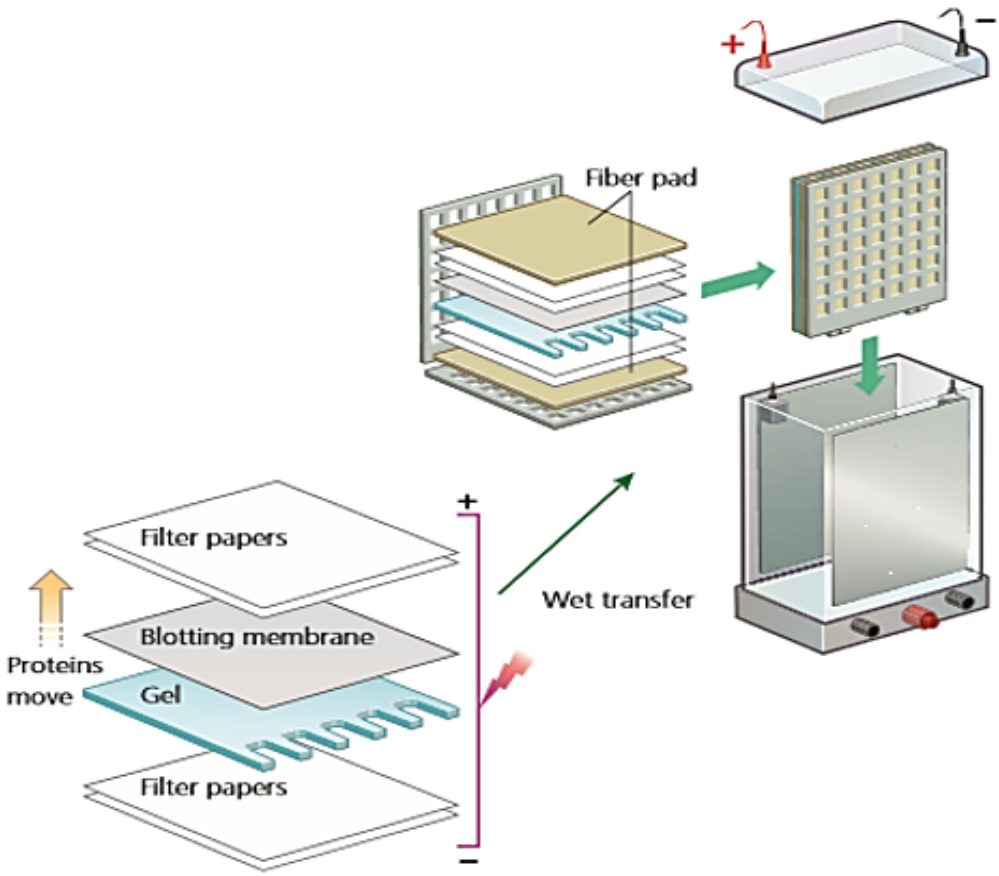

Figure 2.10: Preparation of Wet-transfer Apparatus (http://www.abdserotec.com/westernblotting).

2.12.3 Immunodetection-

After blotting, the target protein was detected using appropriately matched and labelled antibodies. The typical immunodetection stage involves the following steps:

Blocking: The blot containing the transferred protein bands is incubated with a protein or detergent solution which covers the entire surface so that the antibodies do not bind non-specifically to the membrane. The most common blocking solutions contain 3-5% BSA or non-fat dried milk in a solution of Tris-buffered saline. Membranes were blocked with 5% non-fat dry milk (NFDM) in Tris buffer saline (20mM Tris-HCl (pH 7.4), 500mM NaCl and 0.01% Tween 20 (TBST) for 1h.

Antibody incubation- following blocking: Following blocking, the membranes were probed with anti-p53 (AB26, Abcam), anti- bax (AB5714, Abcam), anti-c-PARP (ab11091), anti-Smac/DIABLO, (AB110291, Abcam), anti-Bcl-2 (CS2827, Cell Signalling) and anti-Nrf2 (CS8882, Cell Signalling) diluted to 1:1000 in 5% NFDM in TBST. The membranes were incubated for 1 hr on a shaker at RT and then overnight at 4°C. Since antibody preparations

varied, there was difference in the level of dilution required. As depicted in Figure 2.11, an indirect detection is whereby two different antibodies are used in sequence for the detection step.

Detection with substrate- the label attached to the antibody, usually Horseradish Peroxidase (HRP) is detected using a substrate which produces a visible signal corresponding to the position of the target protein. Membranes were then washed 4 times (10ml TBST, 15min) and treated with horse radish peroxidase (HRP)-conjugated secondary antibody (goat anti-rabbit ; rabbit anti-mouse: 1:10,000 in 5% NFDM, 1h, RT).

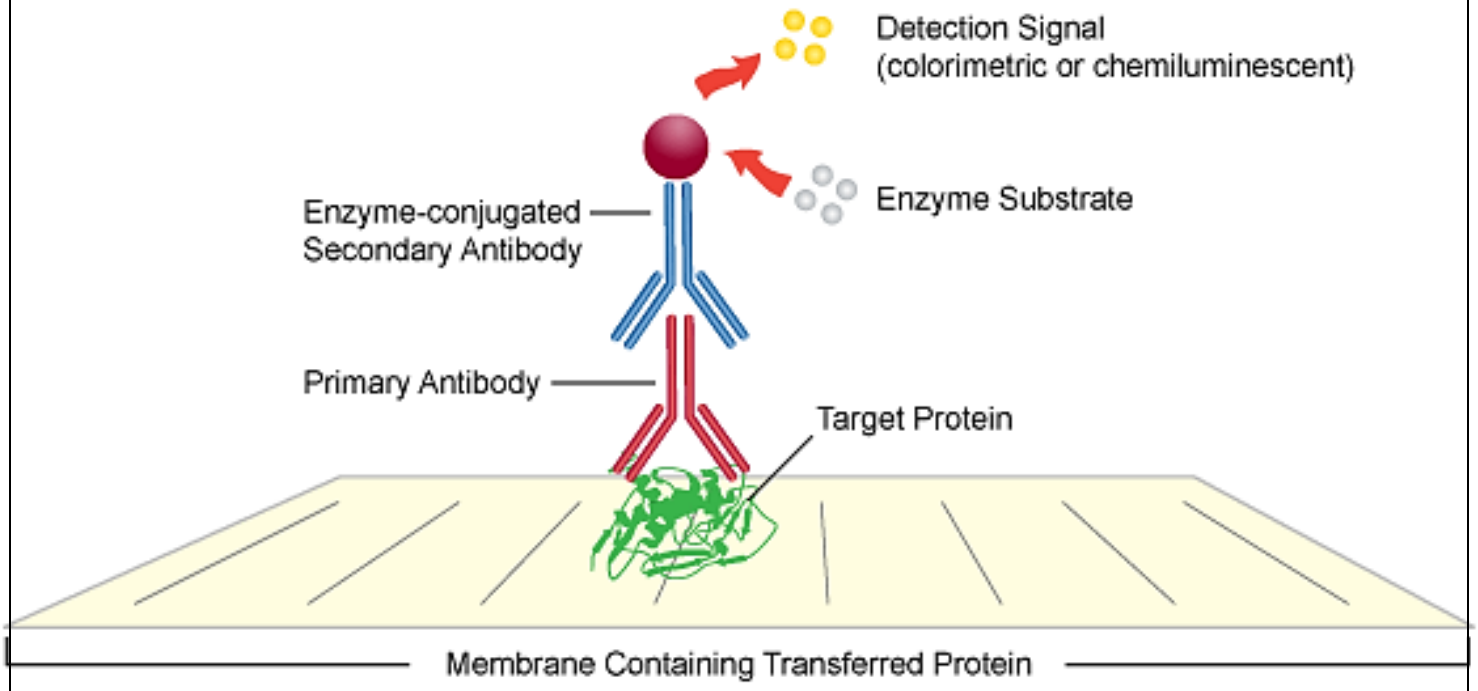

Figure 2.11: Summary of protein Immunodetection using the indirect method (primary and secondary antibody) (http://www.abdserotec.com/westernblotting).

Membranes were washed 4 times (TBST, 15min) and immunoreactivity was detected by Clarity ECL substrate (Biorad). Enhanced chemiluminescence reagents are used for detection. Luminol was oxidized by HRP and an enhancer to produce light. The emitted light was detected by a CCD camera for light capture and was emitted as a band on an imaging system (Taylor, 2014, Mahmood, 2012). Images were captured with the Uvitech Image Documentation System (UViTech Alliance 2.7). Protein bands were analysed with the UViBand Advanced Image Analysis software (UViTech v12.4). Membranes were stripped with 5% hydrogen peroxide

(H_2O_2), rinsed thrice in TTBS, blocked in 5% NFDM (1 h; RT) and probed with HRP-conjugated anti-β-actin (Sigma, St Louis, Missouri, USA). The results were expressed as mean relative band density (RBD), which is relative to the loading control and housekeeping protein β-actin.

2.13 Quantitative Polymerase Chain Reaction:

2.13.1 Introduction-

Polymerase chain reaction (PCR) is the technique used to exponentially amplify a target gene for further analysis. Quantitative reverse transcription PCR (RT-qPCR) is used when the starting material is RNA. In this method, RNA is first transcribed into complementary DNA (cDNA) by reverse transcriptase from total RNA or messenger RNA (mRNA). The cDNA is then used as the template for the qPCR reaction. The two step assay of RT-qPCR is used so that a stable pool of cDNA is made up and stored for multiple reactions. This allows for optimized reaction buffers and reaction conditions to be used.

The principle of PCR is based on the amplification of a segment of DNA using specifically designed primer pairs, deoxynucleoside triphosphates (dNTPs), Taq polymerase, $MgCl_2$ and a buffer solution. Taq DNA polymerase is used to direct the synthesis of DNA from deoxynucleotide substrates on a single-stranded DNA template. Taq polymerase adds nucleotides to the 3' end of a specifically designed oligonucleotide when it is annealed to a longer template DNA, thus the enzyme can use a synthetic oligonucleotide as a primer and elongate its 3' end to generate a region of double stranded DNA (Joshi, 2010, Lilit, 2013).

There are three major steps in PCR, which are repeated for every 30 to 40 cycles. This is done in an automated cycler, which is able to heat and cool tubes with the reaction mixture in a very short time (Figure 2.12).

1. Denaturation- this occurs at 94-96°C and allows for the breakage of weak hydrogen bonds that hold DNA stands together in a helix, allowing the strands to separate creating a single strand.
2. Annealing- the mixture is cooled between 50-70°C. This allows for primers to bind to the complementary sequence in the template DNA. Ionic bonds are constantly formed

and broken between the single stranded primer and single stranded template. The stable bonds allow for the polymerase to attach and copy the template.

3. Extension- The reaction is heated to 72°C, which is the optimal temperature for Taq polymerase. The enzyme extends the primers and adds nucleotides onto the primer in a sequential manner, using the target DNA as a template (Lilit, 2013).

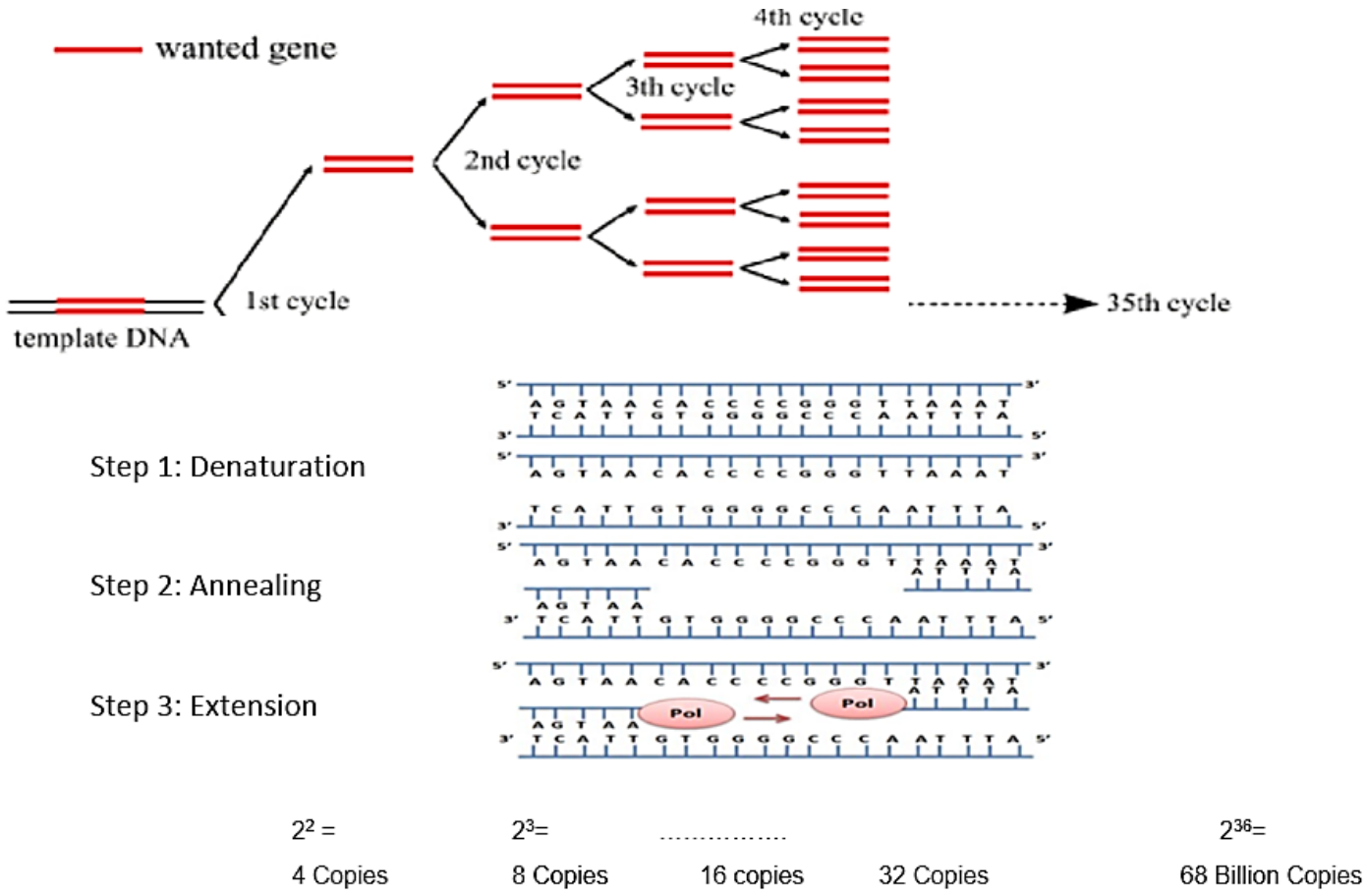

Figure 2.12: Schematic of qPCR principle. With one cycle, a single segment of double stranded DNA template is amplified into two separate pieces of double stranded DNA. These two pieces are then available for amplification in the next cycle. As cycles are repeated, the template is increased exponentially (Adapted from (Nagiah, 2012)).

2.13.2 Protocol-

2.13.2.1 RNA isolation:

RNA was first isolated from the control and ATO treated cells by adding 500µl Qiazol reagent (Qiagen) diluted in 500µl 0.1M PBS and incubated at -80°C for 1h. Chloroform (100µl) was then added and centrifuged (12,000xg, 15min, 4°C). The aqueous upper phase was then removed and added to a new eppendorf followed by the addition of propan-2-ol (250µl, 1h, -

80°C) before centrifugation (12,000xg, 20min, 4°C). Samples were then washed in 75% cold ethanol and centrifuged (7,400xg, 15min, 4°C). Ethanol was then aspirated and RNA pellet was resuspended in 15µl nuclease-free water. Thereafter, RNA was quantified (Nanodrop 2000) and standardised to 1000ng/µl.

2.13.2.2 cDNA Synthesis*:*

A 20µl reaction volume containing 1µl RNA template, 4µl 5X iScript™ reaction mix, 1µl iScript reverse transcriptase and nuclease free water was used to synthesize cDNA (iScript™ cDNA Synthesis kit (BioRad; catalogue no 107-8890). Thermocycler conditions were 25°C for 5min, 42°C for 30min, 85°C for 5min and a final hold at 4°C.

2.13.2.3 Quantitative PCR:

The mRNA expression of *OGG1* (sense: 5'-GCATCGTACTCTAGCCTCCAC-3', anti-sense: 5'-AGGACTTTGCTCCCTCCAC-3') was investigated using Q-PCR. Primer sequences were obtained from Inqaba Biotechnologies. Amplification proceeded in triplicate, in a 25µl reaction consisting of: 12.5µl 5X iScript reaction mix, 2µl of cDNA, 1µl of the primer set and 8.5µl of RNase-free water. Cycling conditions were: initial denaturation (95°C, 4min), 37 cycles of denaturation (95°C, 15s), annealing (57°C, 40s) and extension (72°C, 30s) followed by a plate read for 37 cycles (CFX96 Touch™ Real Time PCR Detection System (Bio-Rad)). The housekeeping gene, Glyceraldehyde-3phosphate dehydrogenase (GAPDH) was run under the same conditions. The analysis of results made use of the method described by Livak and Schmittgen (2001) was used. . Results are expressed as fold change ($2^{-\Delta\Delta Ct}$) relative to the housekeeping gene, GAPDH (sense: 5'-TCCACCACCCTGTTGCTGTA-'3 and anti-sense: 5'-ACCACAGTCCATGCCATCAC-'3) and control (Livak, 2001).

2.14 Statistical Analysis:

Statistical analyses were performed using GraphPad Prism version 5.00 software package (GraphPad PRISM®) and Microsoft excel 2010. Data are expressed as mean ± standard error of the mean (SEM). Comparisons were made using the unpaired Student t-tests using Welch correction. Statistical significance was set at 0.05.

CHAPTER 3:
RESULTS

3.1 Cell Viability:

3.1.1 MTT assay:

The toxicity of ATO to A549 cells was determined using the MTT assay. A dose-response was determined using ATO concentrations in the range 0 to 150µg/ml for 48h (95% Cl=31.34 to 44.68) (Figure 3.1). Analysis of the dose dependent curve showed that 39.25µg/ml ATO was sufficient to cause 50% of A549 cytotoxicity. This IC_{50} concentration was used in all subsequent assays (Cell viability values- Appendix 1).

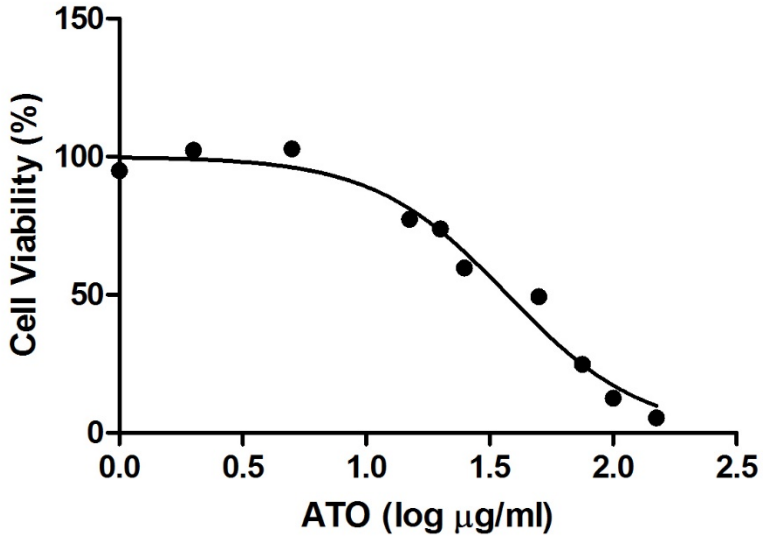

Figure 3.1: Cell viability of A549 cells treated with ATO for 48 hours. Data is represented as a percentage of viable cells relative to the untreated control (0 µM). A dose-dependent decline in A549 cell viability after ATO treatment.

3.1.2 ATP Assay:

Cellular ATP levels were measured using the Cell Titre-Glo® assay. ATO significantly reduced ATP levels with a 3.07-fold decrease (38460 ± 2621 RLU) compared to the control (98050 ± 1751 RLU; p=0.0003) (Figure 3.2) (±: standard deviations from the mean).

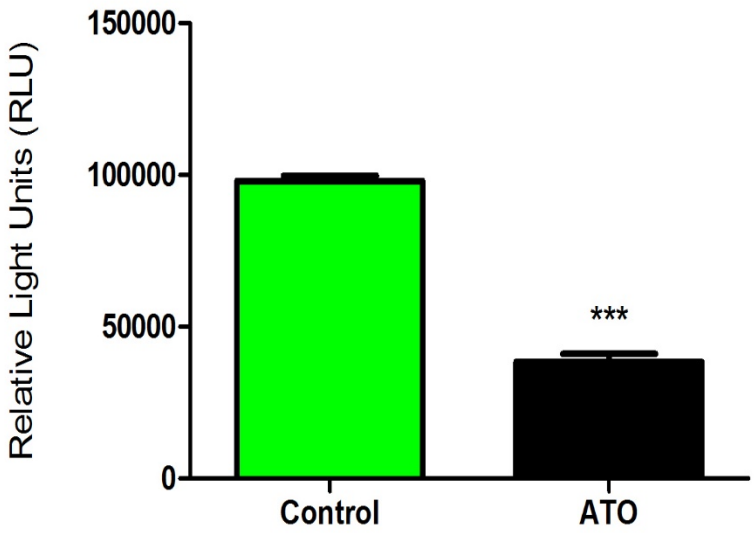

Figure 3.2: ATP levels in ATO treated A549 cells versus Control (*** p≤ 0.001: p=0.0040).

RLU: relative light units.

3.1.3 LDH Assay:

Extracellular levels of LDH were quantified using a colorimetric assay. Results showed a 1.94-fold increase in LDH levels in the supernatant of the ATO treated cells (2.749 ± 0.06714) compared to that of the control supernatant (1.417 ± 0.002496). Results are presented as mean optical density (Figure 3.3) (±: standard deviations from the mean).

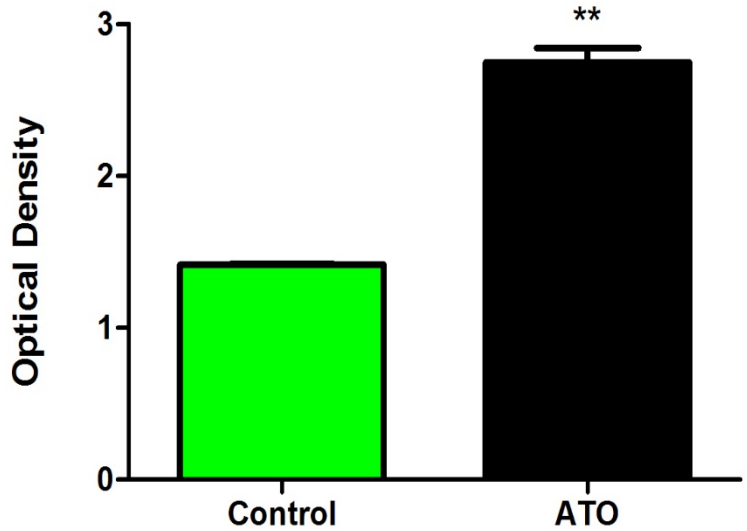

Figure 3.3: Extracellular LDH levels in ATO treated supernatant versus Control (** p≤ 0.01: p=0.0051).

3.2 Oxidative Stress:

3.2.1 Lipid Peroxidation:

Lipid peroxidation, caused by ROS was assessed by quantifying MDA levels (Figure 3.4). The MDA levels were markedly raised in the ATO treated cells (17.62 ± 0.6086) compared to the untreated cells (9.085 ± 0.02261: p=0.0051) (±: standard deviations from the mean).

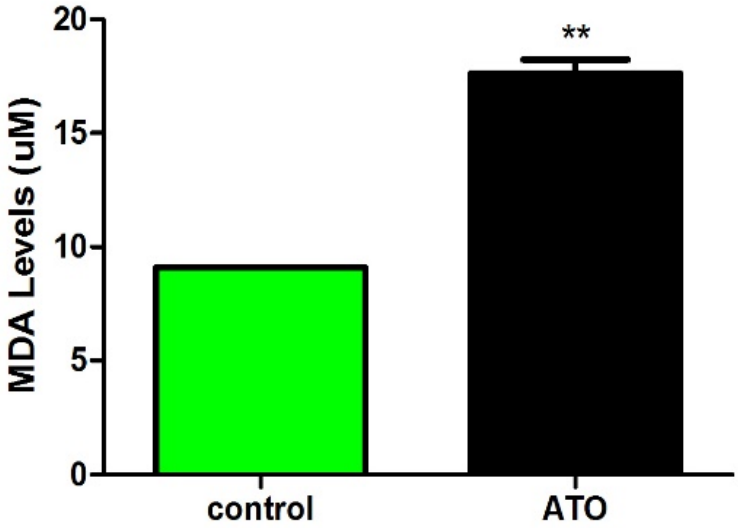

Figure 3.4: Extracellular MDA levels in Control and ATO treatment (** p≤ 0.01: p=0.0051).

3.2.2 Glutathione Assay:

Glutathione (GSH) concentrations were measured using the GSH-Glo™ Glutathione assay as a marker for intracellular anti-oxidant capacity (Figure 3.5). The levels of endogenous antioxidant, GSH, significantly decreased in the ATO treatment compared to the control (571900 ± 14470 RLU vs 348000 ± 9149 RLU: p= 0.0010) (±: standard deviations from the mean).

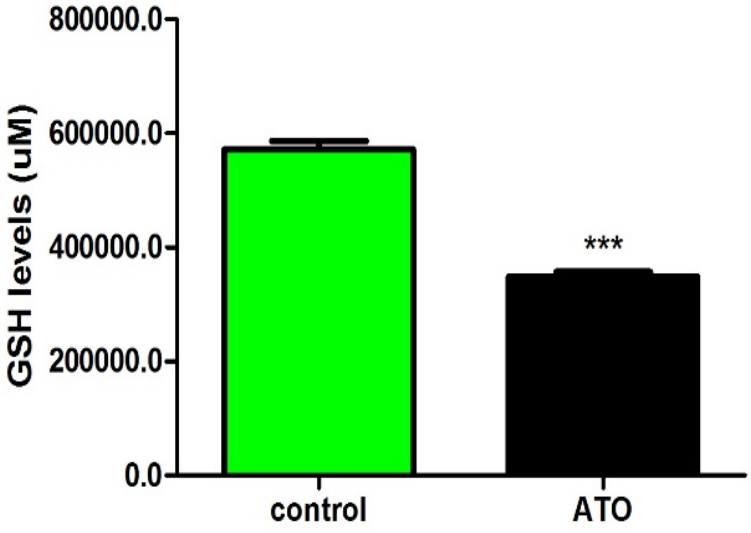

Figure 3.5: Anti-oxidant, GSH, expression in Control and treated cells (*** p≤ 0.001: p=0010).

3.2.3 Nrf2 protein Expression:

Regulator of Antioxidant proteins, Nrf2, expression was measured using Western Blot. Results showed significantly lowered expression (1.29- fold) in the treatment compared to the control (0.1954 ± 0.004683 vs control: 0.2516 ± 0.008478 RBD: p=0.0102). The results of the Nrf2 western blot are reflected as Nrf2 RBD/ β-Actin RBD (Figure 3.6) (±: standard deviations from the mean).

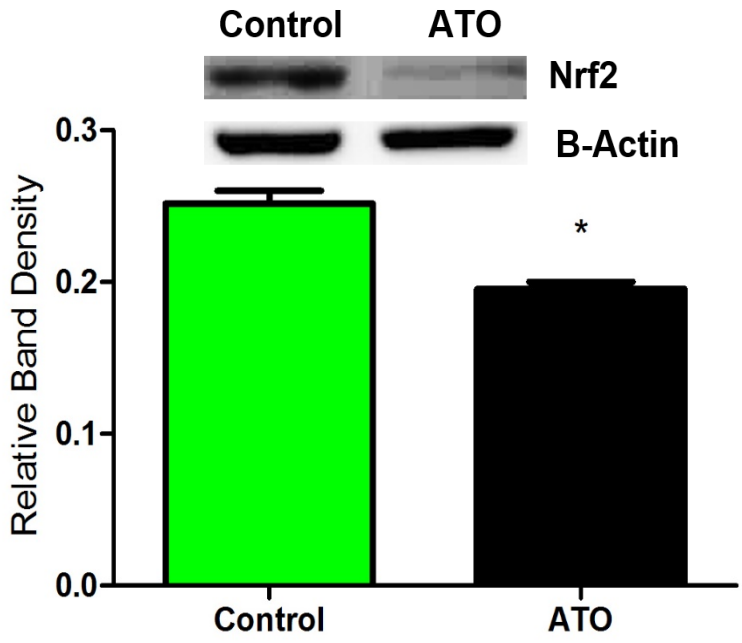

Figure 3.6: Nrf2 expression image and band density graph of control and ATO-treated Protein (* p≤ 0.01: p= 0.0102).

3.3 Apoptosis:

3.3.1 Caspase Activity:

Intracellular activity of caspases -9, -8 and -3/7 were measured. Table 1 represents the apoptotic induction of ATO in A549 cells. There was a significant increase in caspase -9 (1.99-fold), caspase-8 (1.98- fold) and caspase -3/7 (1.66 -fold) activities in the ATO-treated cells compared to the untreated, control cells. Bar graphs shown in Appendix 2 (A-C).

Table 1: Apoptotic Markers of A549 cells following ATO treatment

	Control Mean RLU ± sem	ATO Mean RLU ± sem	p-value
Caspase 9	1832000 ± 1109	2237000 ± 48910	0.0143 (* p≤ 0.01)
Caspase 8	777100 ± 16390	1542000 ± 23940	0.0001 (***p≤ 0.001)
Caspase 3/7	19260 ± 1436	40830 ± 164.7	0.0426 (*p≤ 0.01)

RLU: Relative Light units; sem: Standard error of the mean

3.3.2 Comet Assay:

The comet assay was performed to evaluate DNA fragmentation after ATO exposure. Longer comet tail length is associated with higher DNA fragmentation. Figure 3.7 shows comet tails were significantly longer in the cells treated with ATO compared to the control cells (Figure 3.8), indicating that ATO is genotoxic to A549 cells (19.45 ± 0.5768 vs 19.45 ± 0.5768: $p < 0.0001$) (±: standard deviations from the mean).

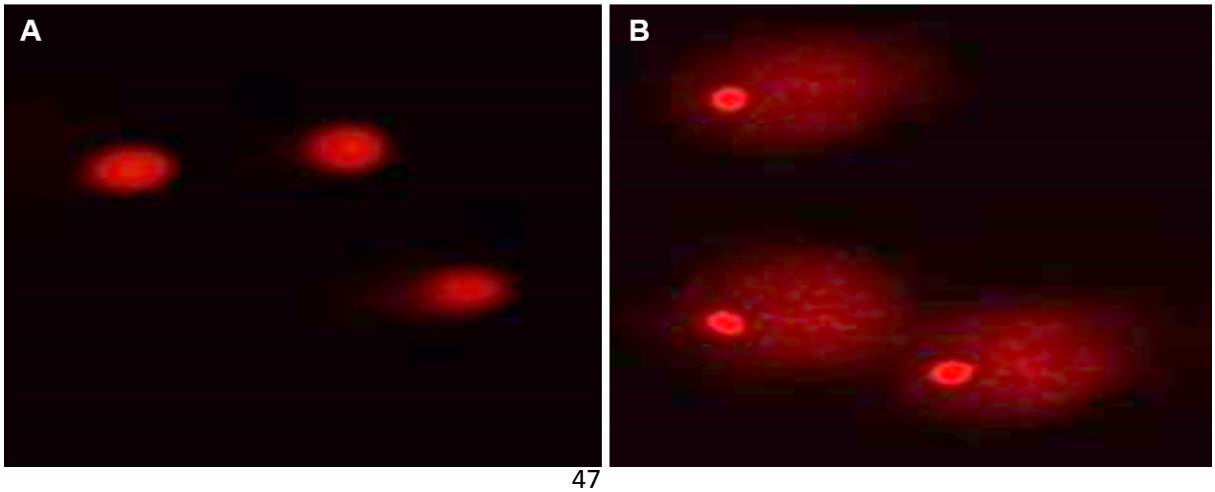

Figure 3.7: Comet tails of A549 cells before exposure to ATO (**A**) and after 48h ATO treatment (**B**) ($p<0.0001$).

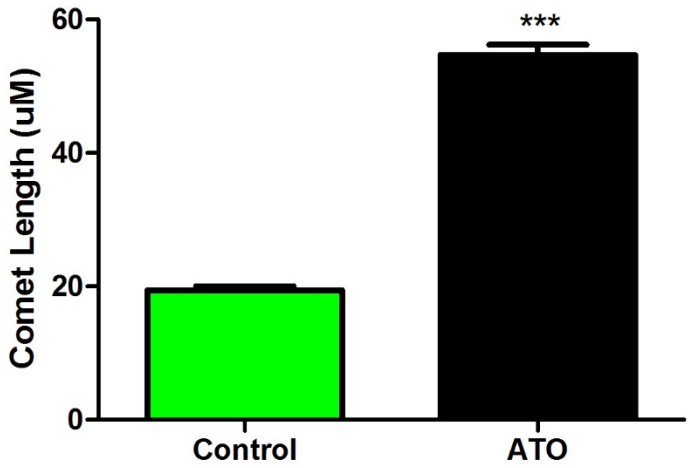

Figure 3.8: Comet tail length was significantly higher in ATO treated cells compared to control (*** $p\leq 0.001$: $p<0.0001$).

3.3.3 Hoechst Assay:

Using the Hoechst stain 33342, the detection of morphological hallmarks of apoptosis were seen including nuclear condensation, cell shrinkage and apoptotic bodies (Figure 3.9 [**B**]). This was compared to the control cells which showed normal cell division at different stages of the cell cycle (Figure 3.9 [**A**]). Cell density was at a lesser extent in the ATO-treated cells compared to the untreated cells.

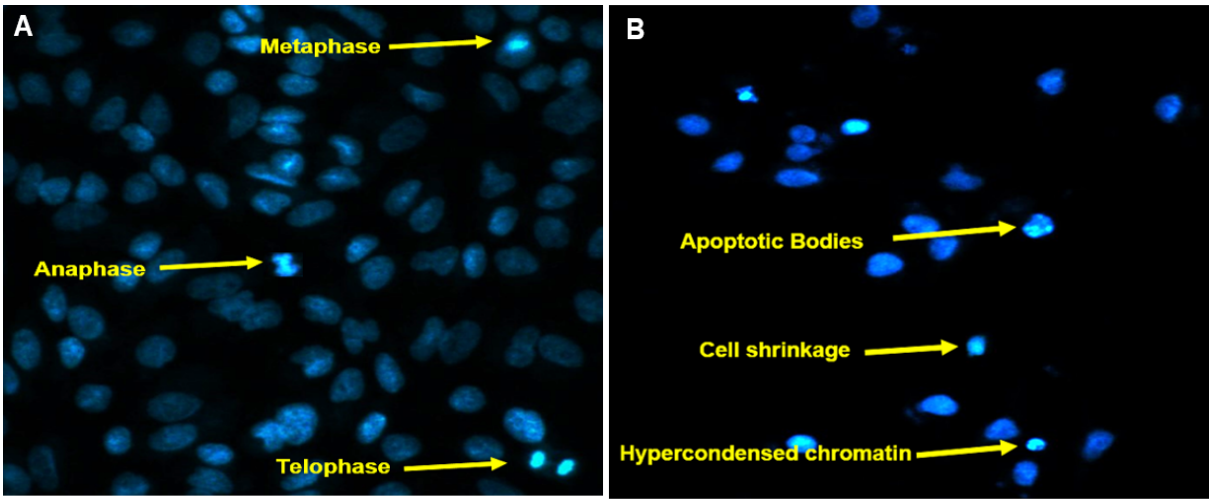

Figure 3.9: Hoechst stained cells show normal cell cycle morphology in A549 control cells (**A**) and apoptotic characteristics in ATO- treated cells (**B**).

3.3.4 DNA repair enzymes- PARP and OGG1:

The mRNA expression of *OGG1* was assessed by qPCR (Figure 3.10). *OGG1* gene expression was significantly diminished (p=0.0363) in the ATO- treatment relative to the normalized control (2.655 ± 0.2089 vs normalized control 1.010 ± 0.005773). The Ct values from the *OGG1* qPCR were used to calculate fold change (±: standard deviations from the mean).Fold change was calculated as $2^{-\Delta\Delta}Ct$ (Appendix 5).

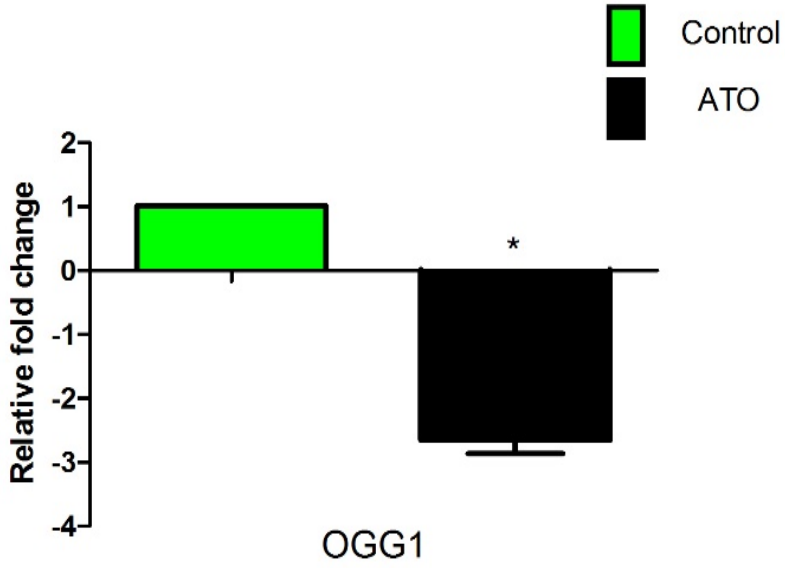

Figure 3.10: *OGG1* mRNA expression was 2.28 fold lower in ATO-induced RNA compared to control (*p≤ 0.01: p=0.0363).

Results for western blot analysis of cleaved PARP yielded an 89kDa and 24kDA fragment (Figure 3.11). Analysis of the fragments showed a 2.39-fold decrease in band intensity of the 89kDA fragment (0.2606 ± 0.0004324 vs control: 0.7329 ± 0.02424 RBD: p=0.0026) and a 1.14 fold increase in expression of the 24kDA fragment (0.5837 ±0.02087 vs control: 0.4705 ± 0.01037 RBD: p=0.0399) (±: standard deviations from the mean).

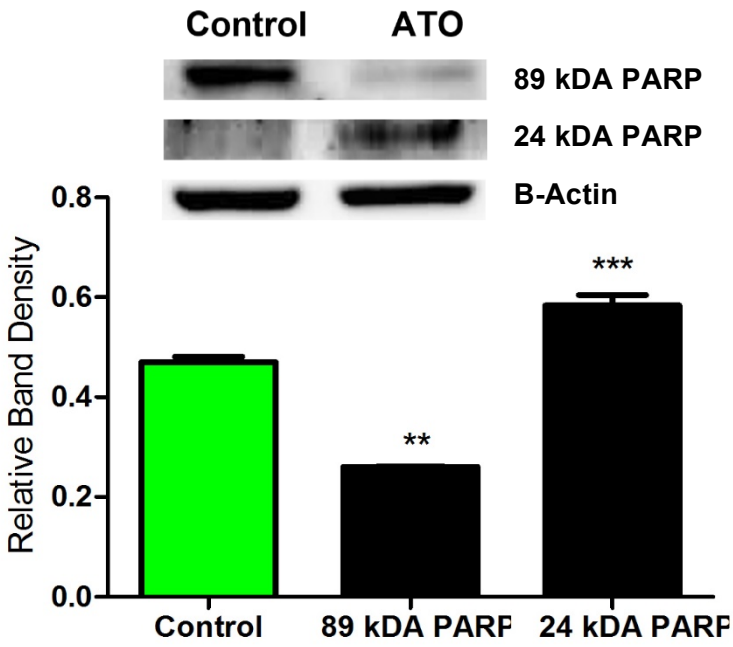

Figure 3.11: Western Blot images and graph of cleaved PARP. Protein expression analysis showed a significant decrease in the 89 kDA fragment (**p≤ 0.001: p=0.0026) and an increase in the 24 kDA fragment (***p≤ 0.0001: p=0.0399).

3.3.5 Apoptotic Markers:

Western blotting was employed to assess the effects of ATO on the protein expression of apoptotic markers Bax, p53, Smac/DIABLO and Bcl-2 (Figure 3.12). ATO induced significant increases in expression of proapoptotic protein Bax (0.3079 ± 0.001639 vs control: 0.1442 ± 0.008411 RBD: fold change- 2.26); tumour suppressor protein p53 (0.5112 ± 0.001380 vs control: 0.3358 ± 0.01474 RBD: fold change- 1.78) and Smac/DIABLO (0.6823 ± 0.02125 RBD vs 0.4615 ± 0.004293 RBD: fold change- 1.35). Anti-apoptotic protein Bcl-2 expressed a 1.21-fold decrease (0.2529 ± 0.001878 vs control: 0.2905 ± 0.01937 RBD: p=0.3039) (±: standard deviations from the mean).

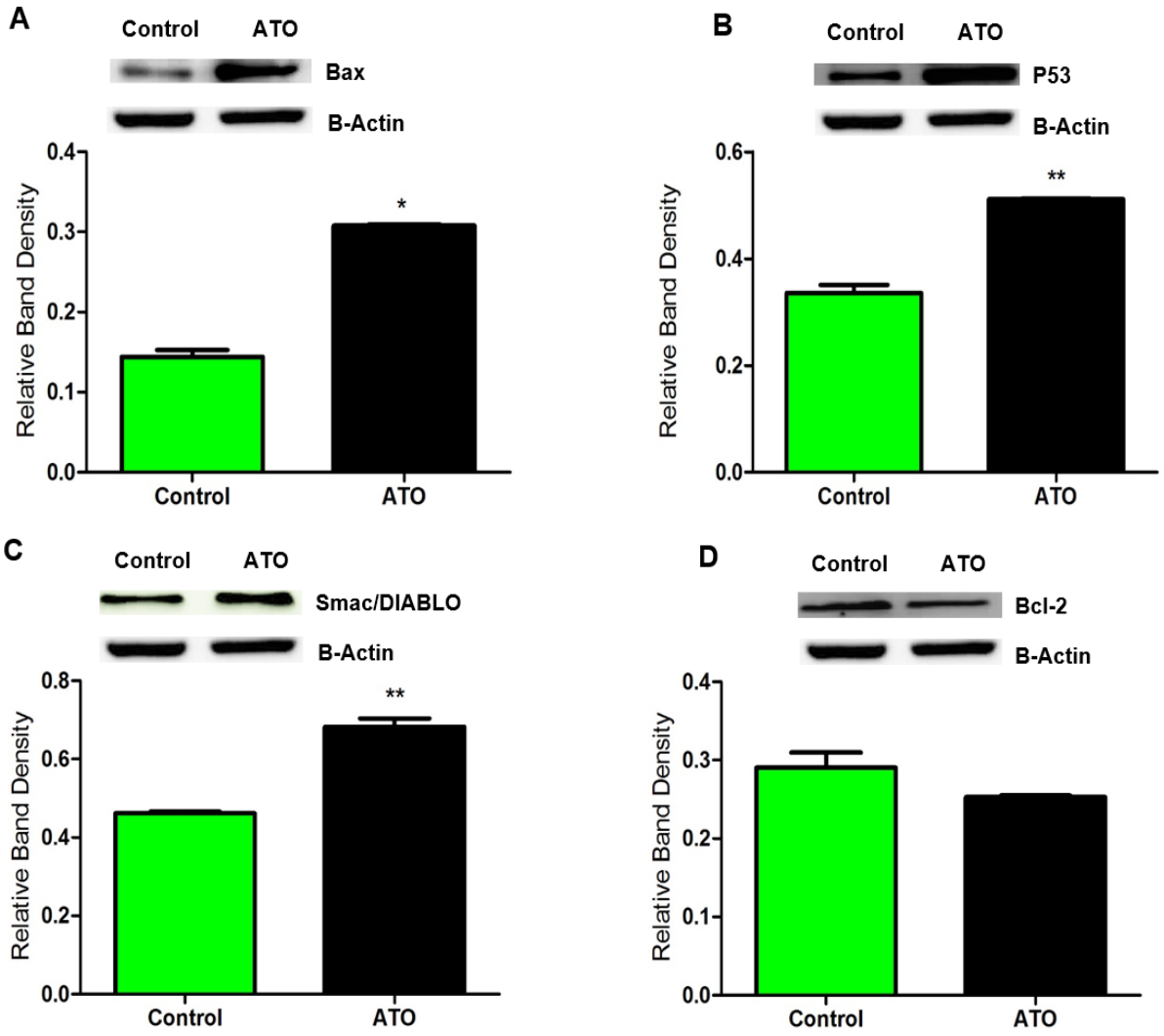

Figure 3.12: Western blot images and band intensity graphs for the expression of (**A**) Bax (*p≤ 0.01: p=0.0333) (**B**) p53 (**p≤ 0.001: p=0.0070) (**C**) Smac/DIABLO (**p≤ 0.001: p=0.0095) and (**D**) Bcl-2 (p=0.3039).

CHAPTER 4:
DISCUSSION

Cancer and heart disease are the major non-communicable causes of death worldwide. Non-small cell lung cancer accounts for approximately 80-85% of all cases of cancer-related mortality in both men and women globally. The major reasons of such high mortality is that NSCLC becomes resistant to chemotherapeutic treatments and radiation therapy. Furthermore, NSCLC is generally diagnosed at very late stages and surgical intervention is not permissible (Siegel, 2012, Molina, 2008).

Systemic anti-cancer therapies, such as chemotherapy, can produce acute and chronic organ damage. In addition, the cost of chemotherapy can be very expensive, thus, it is necessary for improved or novel strategies for lung cancer treatment and prevention by providing therapy with minimal side effects to the patient (Cassileth, 1996).

Statins are inhibitors of HMGCR which prevent cardiovascular disease and lower *LDL* cholesterol. In recent years, the anti-tumour activity of statins, independent of cholesterol reduction, have been established. These anti-tumour properties have been seen in prostate (Lee, 2006), colon (Agarwal, 1999), leukemic (Xia, 2001), pancreatic (Kusama, 2001) and breast cancer cells (Denoyelle, 2001). The positive effects of statins outweigh the minor, asymptomatic adverse effects and are available at an inexpensive cost. Preclinical studies have demonstrated that lipophilic statins (more accessible to tumour cells) such as lovastatin and atorvastatin have better anti-tumour activity, relative to hydrophobic statins such as pravastatin (Cafforio, 2005).

Apoptosis is a succession of precisely regulated events which is altered by cancer cells, leading to cell survival and tumour growth (Fulda, 2009). Therefore, triggering apoptosis can be a promising strategy for cancer chemoprevention.

Our hypothesis on the anti-proliferative properties of ATO on A549 lung cells was formulated on the basis of studies evidencing the pro-apoptotic effects of statins both *in vivo* and *in vitro* (Wong, 2011, Xia, 2001, Agarwal, 1999, Kusama, 2001, Denoyelle, 2001).

Mitochondria are dynamic organelles that constantly undergo adaptations suited to the conditions of the cell; they play a major role in cellular metabolism and are a key source of ROS generation in cells (Hwang, 2013). The inhibition of HMGCR by statins has been linked to mitochondrial dysfunction triggered by increased ROS and decreased prenylated protein

(Tricarico, 2015). In the present study, ATO increased MDA levels (Figure 3.4), a marker of lipid peroxidation induced by increased ROS production.

Under normal physiological conditions ROS regulate intracellular signalling, however, under conditions of excessive ROS production, the endogenous antioxidant system may have been depleted leading to accumulated ROS and increased oxidative damage (Valko, 2006). This imbalance in oxidative stress leads to decreased expression of Nrf2. A direct consequence results in inadequate replenishment of the antioxidant GSH (Shih, 2005). The increase in lipid peroxidation by ATO correlated with decreased Nrf2 protein expression (Figure 3.6) and the significantly decreased GSH levels (Figure 3.5) in the A549 cells.

Cellular targets of ROS include DNA, proteins and phospholipids on cell membranes. ATO increased LDH activity in the culture supernatants (Figure 3.3), a strong indicator of A549 cell membrane damage. The lipophilic nature of ATO is responsible for cell membrane damage. The metabolic function of the A549 cells, after inhibition of HMGCR, was compromised as measured by the dose dependent decrease in MTT conversion (Figure 3.1) and decreased intracellular ATP production (Figure 3.2). The inhibition of HMGCR leads to the accumulation of acetyl-coA in the mt which is converted to citrate and shuttled to the cytosol. This results in decreased reducing equivalents required for ATP production (Diechmann, 2010).

Oxidative stress may be genotoxic to DNA by the modification of purine and pyrimidine bases leading to strand breaks. ROS reacts with DNA bases to form cytotoxic oxidative base lesions, including 7, 8-dihydro-8-oxoguanine (8-oxoG). This oxidised base lesion is different from guanine as it pairs incorrectly with adenine, eventually leading to transversion mutations (Youn, 2007). ATO exposure resulted in DNA damage as evidenced by increased strand breaks and comet tail lengths (Figure 3.7). *OGG1*, a mitochondrial base excision repair enzyme, removes 8-oxoguanine base lesions in both nuclear and mitochondrial genomes, thereby suppressing cell death (Liu, 2011, Ruchko, 2011).

In response to DNA damage, PARP-1 catalyses the poly-ADP-ribosylation of specific nuclear proteins in order to repair DNA strand breaks and overall genomic maintenance (Boulares, 2013, DÁmours, 2001). PARP-1 was cleaved by caspase-3/7 during apoptosis into an 89kDa and 24kDa fragment (Figure 3. 11), thus rendering it inactive.

The genotoxic role of ATO may be attributed to the increase in DNA strand breaks, decreased mRNA expression of *OGG1* and cleavage of PARP-1, thus resulting in cell dysfunction and ultimately apoptosis.

ATO exposure resulted in the initiation of the extrinsic apoptotic pathway as evidenced by increased caspase 8, 3 and 7 (Table 1). The extrinsic apoptotic pathway makes use of transmembrane death receptor- mediated reactions which involve the TNF –α family of death receptors. These death receptors contain death domains and upon ligand binding, recruit adapter FADD via the death domain. Adapter proteins bind to death effector domain-containing caspases-8 giving rise to the formation death inducing signalling complex (DISC), allowing for the activation of caspase 8 which can directly cleave and activate effector caspases 3 and 7 (Johnstone, 2002, Fulda, 2006).

It is interesting to note that caspase 9 was also elevated during our investigation, indicating that the intrinsic apoptotic pathway was simultaneously induced by ATO. During ATO-mediated induction of the intrinsic apoptotic pathway, p53 protein expression was significantly increased (Figure 3.12 **B**) allowing for the transcription and translocation of Bax to the outer mitochondrial membrane while inhibiting anti-apoptotic protein Bcl-2 (Figure 3.12 **D**). This was validated by the significant 2.2 fold increase in Bax protein expression after acute ATO exposure (48 h). A conformational change then occurs and there is depolarization due to a loss in matrix metalloproteinase (MMP). Upon disruption, proteins that were situated within the outer and inner mitochondrial membrane are released into the cytosol including Cytochrome C and Smac/DIABLO (Fulda, 2006, Chai, 2014).

Cytochrome c, together with Apaf1 and pro-caspase 9 form an apoptosome, leading to the cleavage and activation of caspase 9 and executioner caspases which then initiate the morphological hallmarks of apoptosis including a condensed chromatin and apoptotic bodies. This was seen in the Hoechst assay (Figure 3.9) which showed fewer cells and characteristic apoptotic morphology after the ATO treatment.

A class of molecules involved in the regulation of apoptosis is IAP proteins (Fulda, 2006). Inhibitor of apoptosis proteins prevent cell death by suppressing the activity of caspases. Proteins such as Smac/DIABLO activate caspases by facilitating the neutralisation of inhibitors of apoptosis proteins (IAPs). In the cytosol, Smac/DIABLO binds to one molecule of IAP in a BIR-dependent manner to allow for the displacement of caspase 9 from XIAP (Fulda, 2006). ATO increased Smac/DIABLO protein expression (Figure 13.12 **C**) which correlated with the increase in caspase 9 and the initiation of the intrinsic apoptotic pathway.

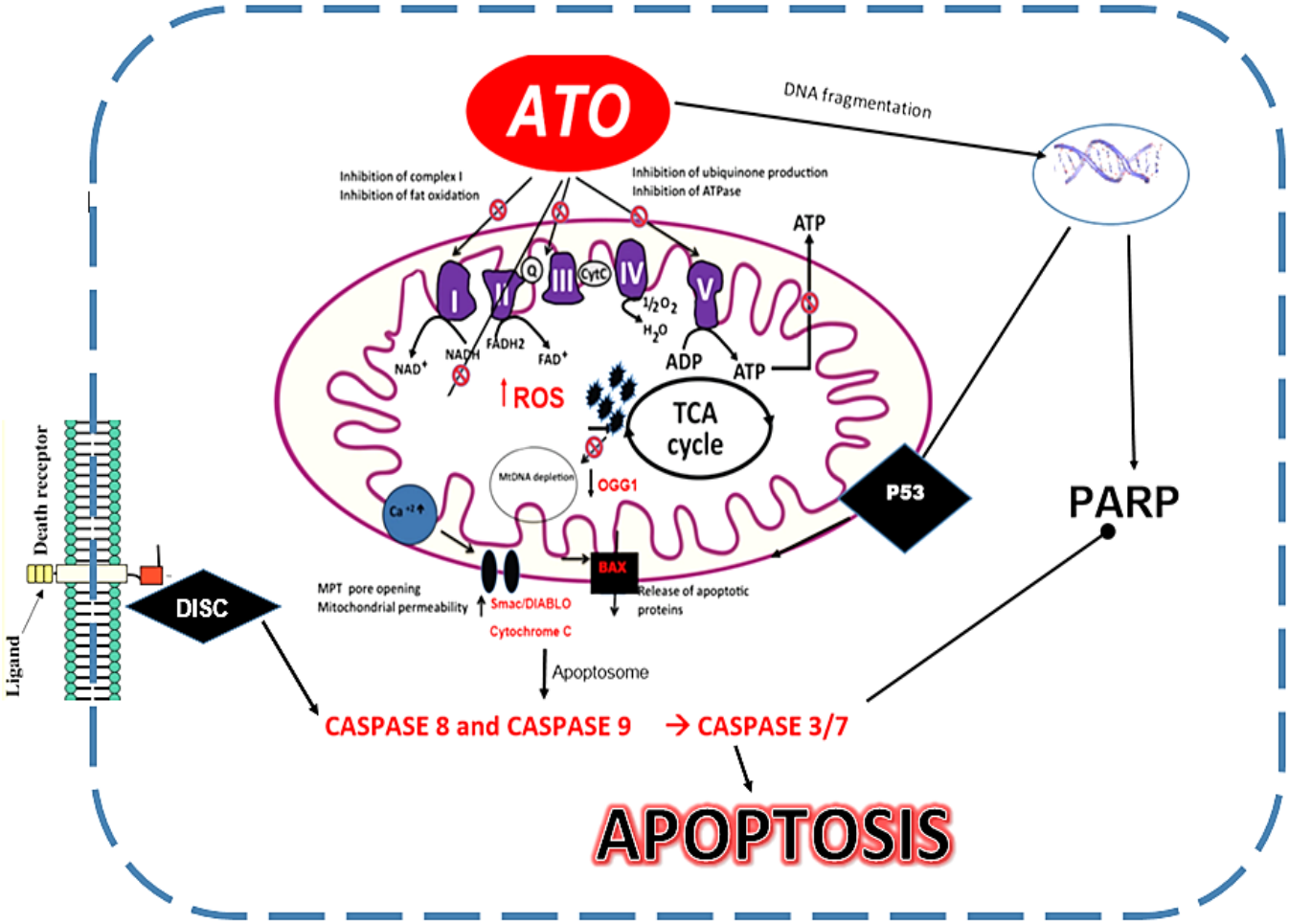

Figure 4: Schematic overview of the apoptosis inducing properties of ATO on human lung adenocarcinoma cells (adapted from Stroes *et al*., 2015).

CHAPTER 5:
CONCLUSION

Current cancer therapies are associated with numerous adverse effects which accentuates the need to develop safer therapies. There is growing evidence from preclinical and clinical investigations that statins may be beneficial in the treatment of malignancies.

In this dissertation, the apoptotic effect of ATO on A549 human non-small lung cancer (NSCLC) cells were demonstrated (Figure 4). ATO was found to exhibit strong growth inhibitory effects on NSCLC cells.

The pro-apoptotic effect of ATO was associated with low ATP availability in A549 cells. This was due to the inhibition of HMGCR, which lead to mitochondrial dysfunction and increased lipid peroxidation. In this study it was shown, mechanistically, that ATO activates the intrinsic and extrinsic apoptotic pathway via caspase 9 and 8 respectively.

Taken together, ATO inhibited lung adenocarcinoma cell survival and promoted apoptosis. Given the importance of the suppression of apoptosis in contributing to tumour growth ad invasion, the drug may have potential in the treatment of lung cancer. Based on the present findings, it would be worthwhile to further investigate the effects of ATO on cell cycle arrest and the consistency of ATO on other cancerous cell lines.

REFERENCES

ADRAIN, C., CREAGH, E.M. AND MARTIN, S.J. 2001. Apoptosis-associated release of Smac/DIABLO from mitochondria requires active caspases and is blocked by Bcl-2. *European Molecular Biology Organization,* 20**,** 6627-6636.

AGARWAL, B., RAO, C. V., BHENDWAL, S., RAMEY, W. R., SHIRIN, H., REDDY, B. S. AND HOLT, P. R. 1999. Lovastatin augments sulindac-induced apoptosis in colon cancer cells and potentiates chemopreventive effects of sulindac. *Gastroenterology,* 117**,** 838-847.

ASHCROFT, M., KUBBUTAT,M.H.G. AND VOUSDEN, K.H. 1999. Regulation of p53 function and stability by phosphorylation. *Cellular Biology,* 19**,** 1751-1758.

BA, X., AGUILERA-AGUIRRE, L., RASHID, Q.T.A.N., BACSI, A., RADAK, Z., SUR, S., HOSOKI, K., HEGDE, M.L., BOLDOGH, I. 2014. The Role of 8-oxoguanine DNA Glycosylase-1 in inflammation. *international Journal of Molecular Science,* 15**,** 16975-16997.

BAJIT, M. L., COVER, C., LEMASTER, J.J. AND JAESCHKE, H 2006. Nuclear translocation of Endonuclease G and Apoptosis-inducing Factor during Acetaminophen-induced liver cell injury. *Toxicological Sciences* 94**,** 217-225.

BARROS, A. L. S., AGUIAR, J.S., ARUAJO, L.C.C., PEIXOTO, C.A., DE MEDEIROS, P.L., CATANHO, M.T.J.A. AND DA SILVA, T.G. 2013. Synergistic anticancer effects of valproic acid, atorvastatin and pioglitazone in human malignant and murine cells. *African Journal of Pharmacy and Pharmacology,* 8**,** 31-39.

BERGMAN, J. 2015. ATP: The Perfect Energy Currency for the cell. *Creation Research Society Quarterly,* 36**,** 1-15.

BOULARES, H. A., YAKOVLEV, A.G., IVANOVA, V., STOICA, B.A., WANG, G., IYER, S. AND SMULSON, M. 2013. Role of Poly(ADP-ribose) Polymerase (PARP) Cleavage in Apoptosis. *The Journal of Biological Chemistry,* 274**,** 22932-22940.

BRENTNALL, M., RODRIGUEZ-MENOCAL, L., DE GUEVARA, R.L., CEPERO, E. AND BOISE, L.H. 2013. Caspase -9, Caspae-3 and Caspase-7 have distinct roles during ntrinsic apoptosis. *BMC- Cell Biology,* 14**,** 1-9.

BROKER, L. E., KRUYT, F.A.E. AND GIACCONE, G. 2005. Cell Death Independent of Caspases: A Review. *Clinical Cancer Research,* 11**,** 3155-3162.

CAFFORIO, P., DAMMACCO, F., GERNONE, A. AND SILVESTRIS,F. 2005. Statins activate the mitochondrial pathway of apoptosis in human lymphoblasts and myeloma cells. *Carcinogenesis,* 26**,** 883-891.

CAIRNS, R. A., HARRIS, I.S. AND MAK, T.W. 2011. Regulation of cancer cell metabolism. *Nature Reviews- Cancer,* 11**,** 85-95.

CANTOR, J. R. A. S., D.M. 2012. Cancer Cell Metabolism: One Hallmark, Many Faces *Cancer Discovery,* 2**,** 881-898.

CASSILETH, B. R. 1996. Alternative and Complementary Cancer Treatments. *The Oncologist,* 1**,** 173-179.

CETINTAS, V. B., KUCUKASLAN, A.S., KOSOVA, B., TETIK, A., SELVI, N., COK, G., GUNDUZ, C. AND EROGLU,Z. 2012. Cisplatin resistance induced by decreased apoptotic activity in non-small-cell lung cancer cell lines. *Cell Biology International,* 36**,** 261-265.

CHAI, J. A. S., Y. 2014. Apoptosome and inflammasome: conserved machineries for caspase activation. *National Science review,* 1**,** 101-118.

CHAN, K. K. W., OZA, A.M., SIU, L.L. 2003. The Statins as Anticancer Agents. *Clinical Cancer Research,* 9**,** 10-19.

CHEN, J., BI, H., HOU, J., ZHANG, X., YUE, L., WEN, X., LIU, D., SHI, H., YUAN, J., LIU, J. AND LIU, B. 2013. Atorvastatin overcomes gefitinib resistance in KRAS mutant human non-small cell lung carcinoma cells. *Cell Death and Disease,* 4**,** 1-13.

COLLARD, T. J., URBAN, B.C., PATSOS, H.A., HAQUE, A., TOWNSEND, P.A., PARASKEVA, C. AND WILLIAMS, A.C. 2012. The Rentinoblastoma protein(Rb) as an anti-apoptotic factor: Expression of Rbis required for the anti-apoptotic function of BAG-1 protein in colorecta ltumour cells. *Cell Death and Disease,* 3**,** 1-9.

DÁMOURS, D., SALLMAN, F.R., DIXIT, V.M.AND POIRIER, G.G. 2001. Gain-of-function of poly(ADP-ribose) polymerase-1 upon cleavage by apoptotic proteases: implications for apoptosis. *Journal of Cell Science,* 114**,** 3771-3778.

DAVIS, W., RONAI, Z.AND TEW, K.D. 2000. Cellular Thiols and Reactive Oxygen Species in Drug Induced Apoptosis. *The Journal of Pharmacology and experimental therapeutics,* 296**,** 1-6.

DENOYELLE, C., VASSE, M., KORNER, M., MISHAL, Z., GANNE, F., VANNIER, J. P., SORIA, J. AND SORIA, C. 2001. Cerivastatin, an inhibitor of HMG-CoA reductase, inhibits the signaling pathways involved in the invasiveness and metastatic properties of highly invasive breast cancer cell lines: an in vitro study. *Carcinogenesis,* 22**,** 1139-1148.

DIECHMANN, R., LAVIE, C. AND ANDREWS, S. 2010. Coenzyme Q10 and Statin-Induced Mitochondrial Dysfunctio. *The Ochsner Journal,* 10**,** 16-21.

DRENT, M., COBEN, N.A.M., HENDERSON, R.F., WOUTERS, E.F.M. AND VAN DIEIJEN-VISSER, M. 1996. Usefulness of lactae dehydrogenase and its isoenzymes as indicators of lung damage or inflammation. *European Respiration Journal,* 9**,** 1735-1742.

ELMORE, S. 2007. Apoptosis: A Review of Programmed Cell Death. *Toxicology Pathology,* 35**,** 495-516.

FISCHER, U. A. S.-O., K. 2006. New Approaches and Therapeutics Targeting Apoptosis in Disease. *Pharmacological Reviews,* 57**,** 187-215.

FOSTER, K. A., OSTER, C.G., MAYER, M.M., AVERY, M.L. AND AUDUS, K.L. 1998. Characterization of the A549 Cell Line as a Type II Pulmonary Epithelial Cell Model for Drug Metabolism. *Experimental Cell Research,* 243**,** 359–366

FRIDMAN, J. S. A. L., S.W. 2003. Control of apoptosis by p53. *Oncogene,* 22**,** 9030-9040.

FULDA, S. 2009. Evasion of Apoptosis as a Cellular Stress Response in Cancer. *International Journal of Cell Biology,* 2010**,** 1-6.

FULDA, S. A. D., K.M. 2006. Extrinsic versus intrinsic apoptosis pathways in anticancer chemotherapy. *Oncogene,* 25**,** 4798-4811.

GAUTHAMAN, K., RICHARDS, M., WONG, J. AND BONGSO, A 2007. Comparative evaluation of the effects of statins on human stem and cancer cells in vitro. *Reproductive Biomedicine Online,* 15**,** 556-581.

GAZDAR, A. F., GIRARD, L., LOCKWOOD, W.W., LAM, W.L., MINNA, J.D. 2010. Lung Cancer Cell Lines as Tools for Biomedical Discovery and Research. *The Journal of the National Cancer Institute,* 102**,** 1310-1321.

GORRINI, C., HARRIS, I.S. AND MAK, T.W. 2013. Modulation of oxidative stress as an anticancer strategy. *Nature Reviews,* 12**,** 931-947.

GOVENDER, R., PHULUKDAREE, A., GENGAN, R.M., ANAND, K. AND CHUTURGOON, A.A. 2012. Silver nanoparticles of Albizia adianthfolia: the induction of apoptosis in a human lung carcinoma cell line. *Masters Thesis*.

GUENGERICH, F. P. 1993. Cytochrome P450 Enzymes. *American Scientist,* 81**,** 440-447.

HEIDEN, M. G. V., CANTLEY, L.C. AND THOMPSON, C.B. 2009. Understanding the Warburg effect: he Metabolic requirements of cell proliferation. *Science,* 324**,** 1029-1033.

HIGGENBOTTAM, T., SHIPLEY, M.J. AND ROSE,G. 1982. Cigarettes, lung cancer, and coronary heart disease: the effects of inhalation and tar yield. *Journal of Epidemiology and Community Health,* 36**,** 113-117.

HINDLER, K., CLEELAND, C.S., RIVERA, E. AND COLLARD, C.D. 2006. The Role of Statins in Cancer Therapy. *The Oncologist,* 11**,** 306-315.

HOQUE, A., CHEN, H. AND XU, X. 2008. Statin Induces Apoptosis and Cell Growth Arrest in Prostate Cancer Cells. *Cancer Epidemiology Biomarkers,* 17**,** 88-94.

HSU, H., XIONG, J. AND GOEDDEL, D.V. 1995. The TNF Receptor I-Associated Protein TRADD Signals. Cell Death and NF-KB Activation *Cell,* 81**,** 495-504.

HWANG, K., PARK, C., KWON, S., KIM, Y., PARK, D., LEE, M., KIM, B., PARK, S., YOON, K., JEONG, E. AND KIM, H 2013. Synergistic induction of apoptosis by sulindac and simvastatin in A549 human lung cancer cells via reactive oxygen species-dependent mitochondrial dysfunction. *International Journal of Oncology,* 43**,** 262-270.

ISTVAN, E. S. A. D., J. 2001. Structural mechanism for statin inhibition of HMG-CoA reductase. *Science,* 292**,** 1160-1164.

JASTROCH, M., DIVAKARUNI, A.S., MOOKERJEE, S., TREBERG, J.R. AND BRAND, M.D. 2010. Mitochondrial proton and electron leaks. *Essays Biochemistry,* 2010**,** 53-67.

JAVIE, M. A. C., N.J. 2011. the Role of PARP in DNA repair and its Therapeutic exploitation. *British Journal of Cancer,* 105**,** 1114-1122.

JOHNSTONE, R. W., RUEFLI, A.A. AND LOWE, S.W. 2002. Apoptosis: A Link between Cancer Genetics and Chemotherapy. *Cell* 106**,** 153-164.

JOSHI, M. A. D., J.D. 2010. Polymerase chain reaction: Methods, principles and application. *International Journal of Biomedical Research,* 1**,** 81-97.

KERR, J. F., WYLLIE, A.H. AND CURRIE, A.R. 1972. Apoptosis: a basic biological phenomenon with wide-ranging implications in tissue kinetics. *British Journal of Cancer,* 26**,** 239-257.

KRACIKOVA, M., AKIRI, G., GEORGE, A., SACHIDANANDAM, R. AND AARONSON, S.A. 2013. A threshold mechanism mediates p53 cell fate decision between growth arrest and apoptosis. *Cell Death and Differentiation,* 20**,** 576-588.

KUSAMA, T., MUKAI, M., IWASAKI, T., TATSUTA, M., MATSUMOTO, Y., AKEDO, H. AND NAKAMURA, H. 2001. Inhibition of epidermal growth factor-induced RhoA translocation and invasion of human pancreatic cancer cells by 3-hydroxy-3methylglutaryl-coenzyme a reductase inhibitors. *Cancer Research,* 61**,** 4885-4891.

LEE, J., LEE, I., PARK, C. AND KANG, W. K. 2006. Lovastatin-induced RhoA modulation and its effect on senescence in prostate cancer cells. *Biochemical and Biophysical Research Communications,* 339**,** 748-754.

LILIT, G. A. N., A. 2013. Polymerase Chain Reaction. *Journal of Investigative Dermatology,* 133**,** 1-4.

LIU, G. A. K., D.W. 2011. Mitochondrial DNA Damage: Role of Ogg1 and Aconitase. *DNA Repair***,** 85-102.

LIVAK, K. J. A. S., T.D. 2001. Analysis of relaive gene expression data using real-time quantitative PCR and the 2(-Delta Delta C(T)) method. *methods,* 25**,** 402-408.

MAHMOOD, T. A. Y., P. 2012. Western Blot: Technique, Theory, and Trouble Shooting. *North American Journal of Medical Sciences,* 4**,** 429-434.

MARTINEZ-RUIZ, G., MALDONADO, V., CEBALLOS-CANCINO, G., GRAJEDA, J.P.R. AND MELENDEZ-ZAJGLA, J. 2008. Role of Smac/Diablo in cancer progression. *Journal of Experimental & Clinical Cancer Research,* 27**,** 1-7.

MÁTES, J. M., SEGURA, J.A., ALONSO, F.J. AND MÁRQUEZ, J. 2012. Oxidative stress in apoptosis and cancer: an update. *Archives of Toxicology,* 10**,** 1-17.

MCMURRAY, C. T. 2010. Mechanisms of Trinucleotide repeat instability during human development. *Nature Reviews Genetics,* 11**,** 786-799.

MEHTA, R. G. 2014. Currrent paradigms of cancer chemoprevention. *Turkish Journal of Biology,* 38**,** 839-847.

MITSUISHI, Y., MOTOHASHI, H., YAMAMOTO, M. 2012. The Keap1-Nrf2 system in cancers: Stress response and anabolic metabolism. *frontiers in oncology: Molecular and Cellular Oncology,* 2012.

MOLINA, J. R., YANG, P., CASSIVI, S.D., SCHILD, S.E. AND ADJEI, A.A. 2008. Non–Small Cell Lung Cancer: Epidemiology, Risk Factors, Treatment, and Survivorship. *Mayo Clinic Proceedings,* 83**,** 584-594.

MUKANSI, M., SMITH, C. AND FELDMAN, C 2014. A study of lung cancer in Johannesburg, South Africa. *The Southern African Journal of Epidemiology and Infection,* 29**,** 43-47.

MYLONAS, C. A. K., D. 1999. Lipid Peroxidation and Tissue damage. *In Vivo,* 13**,** 295-309.

NAGIAH, S. 2012. The role of uncoupling protein2-866G/A polymorphism in oxidative stress markers associated with air pollution exposure during pregnancy. *(Masters Thesis)*.

NODA, N. A. W., H. 2001. Cancer and Oxidative Stress. *Japan Medical Association Journal,* 44**,** 535-539.

OKA, M., MAEDA, S., KOGA, N., KATO, K. AND SAITO, T. 1992. A Modified Colorimetric MTT Assay Adapted for Primary Cultured Hepatocytes: Application to Proliferation and Cytotoxicity Assays. *Bioscience, Biotechnology and Biochemistry,* 56**,** 1472-1473.

OLA, M., NAWAZ, M. AND AHSAN, H. 2011. Role of Bcl-2 family proteins and caspases in the regulation of apoptosis. *Molecular Cell Biochemistry,* 351**,** 41-58.

OLIVE, P. L. A. B., J.P. 2006. The comet assay: a method to measure DNA damage in individual cells. *Nature Protocols,* 1**,** 23-29.

PACELLA-NORMAN, R., URBAN, M.I., SITAS, F., CARRARA, H., SUR, R., HALE, M., RUFF, P., PATEL, M., NEWTON, R., BULL, D. AND BERAI, V 2002. Risk factors for oesophageal, lung, oral and laryngeal cancers in black South Africans. *British Journal of Cancer,* 86**,** 1751-1756.

PISANTI, S., PICARDI, P., CIAGLIA, E., DÁLESSANDRO, A. AND BIFULCO, M. 2014. Novel Prospects of Statins as Therapeutic Agents in Cancer. *Pharmacological Research,* 88**,** 84-98.

POWERS, S. K. A. J., M.J. 2008. Exercise-Induced Oxidative Stress: Cellular Mechanisms and Impact on Muscle Force Production. *Physiological Reviews,* 88**,** 1243-1276.

RAHMAN, I. A. M., W. 1999. Lung Glutathione and oxidative stress: Implications in cigarette smoking-induced airway disease. *The American Physiological Society,* 99**,** 1-22.

RASTOGI, R. P., SINHA, R. AND SINHA, R.P. 2009. Apoptosis: Molecular Mechanisms and Pathogenicity. *EXCLI Journal,* 8**,** 155-181.

RIECKHER, M., AND TAVERNARAKIS, N 2010. Caspase-Independent Cell Death Mechanisms in Simple Animal Models. *Programmed cell death mechanisms***,** 9-32.

RIGNANTI, C., PINTO, H., BOLLI, E., BELISARO, D.C., CALOGERO, R.A., BOSIA, A. AND CAVALLO, F. 2011. Atorvastatin modulates anti-proliferative and pro-proliferative signals in Her2/neu-possitive mammary cancer. *Biochemical Pharmacology,* 82**,** 1079-1089.

RISS, T. L., MORAVEC, R.A., NILES, A.L., BENINK, H.A., WORZELLA, T.J., MINOR, L., STORTS, D. AND REID, Y. 2013. Cell Viability Assays. *Assay Guidance Manual* 1-23.

RUCHKO, M. V., GORODNYA, O.M.M ZULETA, A., PASTUKH, V.M. AND GILLESPIE, M.N. 2011. The DNA Glycosylase, Ogg1, Defends Against Oxidant-induced mtDNA Damage and Apoptosis in Pulmonary Artery Endothelial Cells. *Free radical Biology Medicine* 50**,** 1107-1113.

SEXTON, K., BALHARRY, D. AND BERUBE, K. A. 2008. Genomic biomarkers of pulmonary exposure to tobacco smoke components. *Pharmacogenetics and Genomics,* 18**,** 853-860.

SHIH, A. Y., LI, P. AND MURPHY, T.H. 2005. A Small-Molecule-Inducible Nrf2-Mediated Antioxidant Response Provides Effective Prophylaxis against Cerebral Ischemia In Vivo. *the Journal Of Neuroscience,* 25**,** 10321-10335.

SIEGEL, R., NAISHADHAM, D. AND JEMAL, A. 2012. Cancer Statistics 2012. *CA: A cancer journal for Clinicians,* 62**,** 10-29.

SMITH, P. K., KROHN, R.I., HERMANSON, G.T., MALLIA, A.K., GARTNER, F.H., PROVENZANO, M.D., FUJIMOTO, E.K., GOEKE, N.M., OLSON, B.J. AND KLENK, D.C. 1985. Measuremnt of Protein Using bicinchoninic acid. *Analytical Biochemistry,* 150**,** 76-85.

STANCU, C. A. S., A. 2001. Statins: Mechanism of action and effects. *Journal of cellular and molecular Medicine,* 5**,** 378-387.

STEIN, L., URBAN, M.I., WEBER, M., RUFF, P., HALE, M., DONDE, B., PATEL, M. AND SITAS, F. 2008. Effects of tobacco smoking on cancer and cardiovascular disease in urban black South Africans. *British Journal of Cancer,* 98**,** 1586-1592.

STROES, E. S., THOMPSON, P.D., CORSINI, A., VLADUTIU, G.D., RAAL, F.J., RAY, K.K., RODEN, M., STEIN, E., TOKGOZOG˘LU, L., NORDESTGAARD, B.J., BRUCKERT, E., BACKER, G., KRAUSS, R,M., LAUFS, U., SANTOS, R.D., HEGELE, R.A., HOVINGH, G.K., LEITER, L.A., MACH, F., MARZ, W., NEWMAN, C.B., WIKLUND, O., JACOBSON, T.A., CATAPANO, A.L., CHAPMAN, M.J. AND GINSBERG, H.N. 2015. Statin-associated muscle symptoms: impact on statin therapy- European Atherosclerosis Society Consensus Panel Statement on Assessment, Aetiology and Management. *European Heart Journal***,** 1-13.

TANDON, V., BANO, G., KHAJURIA, V., PARIHAR, A. AND GUPTA, S. 2004. Pleitropic Effects of Statins. *Indian Journal of Pharamacology,* 37**,** 77-85.

TAYLOR, S. C. A. P., A. 2014. The design of a quantitative Western blot Experiment. *BioMed Research international,* 2014**,** 1-8.

TRICARICO, P. M., CROVELLA, S., CELSI, F. 2015. Mevalonate Pathway Blockade, Mitochondrial Dysfunction and Autophagy: A Possible Link. *International Journal of Molecular Science,* 16**,** 16067-16084.

VALKO, M., RHODES, C.J., MONCOL, J., IZAKOVIC, M. AND MAZUR, M. 2006. Free radicals, metals and antioxdants in oxidative stress-induced cancer. *chemico-Biological interactions,* 160.

VEKSHIN, N. 2011. Bindingof Hoechst with Nucleic Acids using Fluorescence spectroscopy. *Journal of Biophysical Chemistry,* 2**,** 443-447.

VERHOEF, M. J., ROSE, M.S., WHITE, M. AND BALNEAVES, L.G. 2008. Declining Conventional cancer treatment and using complementary and alternative medicine: a problem or a challenge? *Current Oncology,* 15**,** 101-106.

WANG, X. 2001. The expanding role of mitochondria in apoptosis. *Genes and Development,* 15**,** 2922-2933.

WANG, Y., SOLT, L.A., KOJETIN, D.J. AND BURRIS, T.P. 2012. Regulation of p53 Stability and Apoptosis by a ROR Agonist. *Plos One,* 7**,** 1-6.

WONG, R. S. Y. 2011. Apoptosis in cancer: from pathogenesis to treatment. *Wong Journal of Experimental & Clinical Cancer Research,* 30**,** 1-14.

WONG, W. W. L., DIMITRITROULAKOS, J., MINDEN, M.D. AND PEN, L.Z. 2002. HMG-CoA reductase inhibitors and the malignant cell: the statin family of drugs as triggers of tumor-specific apoptosis *Leukemia,* 16**,** 508-519.

XIA, Z., TAN, M. M., WONG, W. W., DIMITROULAKOS, J., MINDEN, M. D. AND PENN, L. Z. 2001. Blocking protein geranylgeranylation is essential for lovastatin-induced apoptosis of human acute myeloid leukemia cells. *Leukemia* 15**,** 1398-1407.

YOKOTA, J. 2000. Tumour progression and metastasis. *Carcinogenesis,* 21**,** 497-503.

YOUN, C., SONG, P.I., KIM, M., KIM, J.S., HYUN, J., CHOI, S., YOON, S.P., CHUNG, M.H., CHANG, I. AND YOU, H.J. 2007. Human 8-Oxoguanine DNA Glycosylase Suppresses the Oxidative Stress–Induced Apoptosis through a p53-Mediated Signaling Pathway in Human Fibroblasts. *Molecular Cancer Research,* 1083-1098.

YU, J., YUE, W., WU, B. AND ZHANG, L. 2006. PUMA Sensitizes Lung Cancer Cells to Chemotherapeutic agents and Irradiation. *Clinical Cancer Research,* 12**,** 2928-2937.

APPENDICES

APPENDIX 8.1

Table 1: Raw data for the determination of IC_{50} using the cell viability (MTT) assay.

ATO Concentration (µg/ml)	Average Absorbance	% Viability	Log [ATO]
0	1,426	100,00	
1	1,354	94,95	0,000
2	1,459	102,31	0,301
5	1,466	102,78	0,699
10	1,603	112,41	1
15	1,102	77,28	1,176
20	1,053	73,87	1,301
25	0,851	59,70	1,398
50	0,703	49,32	1,699
75	0,355	24,87	1,875
100	0,180	12,62	2,000
150	0,078	5,49	2,176

APPENDIX 8.2

Table of Components Present in Eagles Minimum Essentials Media

COMPONENT	CONCENTRATION
Inorganic Salts	
$CaCl_2.2H_2O$	186,0
KCL	400,0
KH_2PO_4	60,0
$MgSO_4.7H_2O$	200,0
NaCl	8000,0
$NaHCO_3$	350,0
$Na_2HPO_4.7H_2O$	90,0
Other Components	
Glucose	1000,0
Phenol Red	20,0
Amino Acids	
L-Arginine-HCl	126,4
L-Cysteine	24,0
L-Histidine-HCl.H_2O	42,0
L-Isoleucine	52,4
L-Leucine	52,4
L-Lysine-HCl	73,0
L-Methionine	15,0
L-Phenylalanine	33,0
L-Threonine	47,6
L-Tryptophan	10,2
L-Tyrosine	47,6
L-Valine	46,8
Vitamins	
D-Capantothenate	1,0
Choline Chloride	1,0
Folic acid	1,0
i-Inositol	2,0
Nicotinamide	1,0
Pyridoxine	1,0
Riboflavin	0,1

Thiamine-HCl	1,0

APPENDIX 8.3

Caspase Activity: Graphs

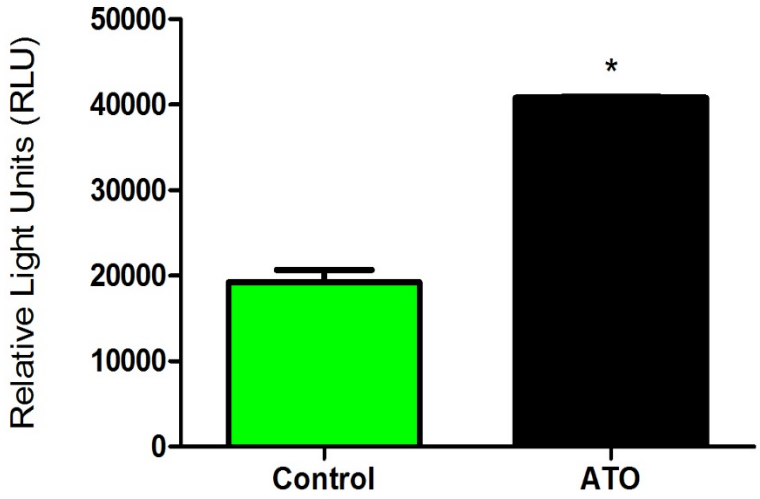

Figure 1: Caspase-3/-7 activity was significantly higher in cells exposed to ATO compared to untreated cells (p=0.0426).

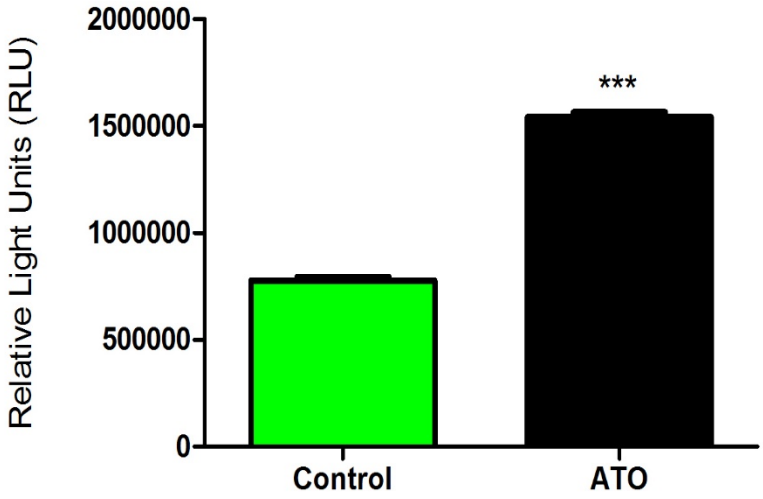

Figure 2: The activity of caspase-8 was significantly increased in cells exposed to ATO compared to untreated cells (p=0.0001).

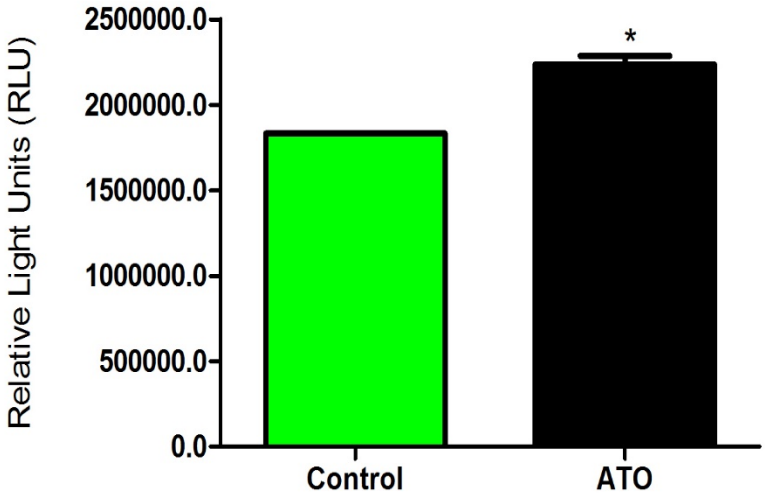

Figure 3: ATO caused a significant increase in the activity of caspase-9 compared to control cells (p=0.0143).

APPENDIX 8.4

Protein Standards BSA (mg/ml)	0	0,2	0,4	0,6	0,8	1
OD1	0,101	0,229	0,422	0,64	0,823	0,963
OD2	0,105	0,248	0,429	0,603	0,764	0,892
OD3	0,1	0,302	0,44	0,533	0,757	0,967
Average	0,102	0,260	0,430	0,592	0,781	0,941

Table 1: Protein Quantification and Standardisation using Bovine Serum Albumin (BSA)

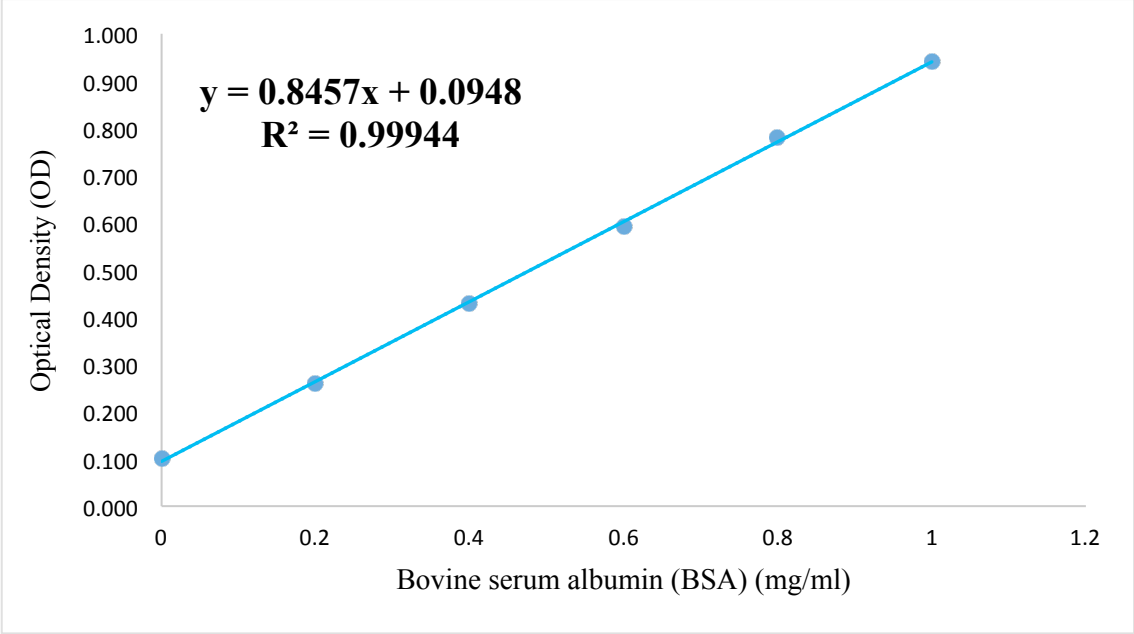

Figure 1: Calibration curve using known concentrations of bovine serum albumin for the determination of protein concentration in samples using the bicinchoninic acid assay

Table 2: Standardisation of protein using the calibration curve for sodium dodecyl sulphide polyacrylamide gel electrophoresis.

	Average Absorbance	Protein (mg/ml)	C2 (mg/ml)	V2 (µl)	V1(µl)
Control	1,521	1,686	0.800	200	94,899
ATO	0,838	0,879	0.800	200	182,025

APPENDIX 8.5

The $2^{-\Delta\Delta CT}$ Method for Analysis of quantitative PCR

The 2-ΔΔCt method refers to the method of analysis used to obtain a relative fold change of a treated sample compared to an appropriate control group as described by Livak and Schmittgen (2001).

Equations:

ΔC (t) = Gene (Ct) – Housekeeping gene (Ct)

ΔΔC (t) = Experimental group (ΔCt) – Control (ΔCt)

Fold change = $2^{-\Delta\Delta C(t)}$

Control	*Control*	*Control*	*ATO*	*ATO*	*ATO*
			OGG1		
27,73	28,00	27,82	28,47	28.27	29,09
			GAPDH		
9,89	9,80	9,55	9,08	9,55	9,47
			ΔC(t)		
17,83	18,20	18,27	19,39	18,73	19,62
Average Control					
			18,10		
			ΔΔC(t)		
0,27	0,10	0,17	1,29	0,62	1,52
			Fold change		
1,204017	0,933841	0,889394	0,408726	0,649107	0,349117